SHEAR TRANSFER OF LOAD FROM MAIN BEAMS TO INTERMEDIATE CORRUGATIONS IN METAL SHEET COVERED BOX BEAMS

Thesis by

G.R.Mellinger
and
H.Kurihara

In Partial Fulfillment of the Requirements for
the Degree of Master of Science in Aeronautical Engineering

California Institute of Technology
Pasadena, California
1938

TABLE OF CONTENTS

I. SUMMARY

A program of experimental investigation for three combinations of sheet reenforced with corrugations has been carried out.

An assumption has been made for the transverse neutral axis of such a system.

For an open section box beam, the conventional assumption of the neutral axis on the center of gravity plane indicates an error.

An attempt has been made to calculate the compressive stress in each corrugation due to shear transfer of load.

An effective shear modulus for each corrugation and its share of the skin under bending loads has been found by experimental methods.

For the combinations tested, it was found that the effective shear modulus, G/E, decreases with increasing τ, which corresponds to increasing G/E with distance from the free end of the panel.

Panel curvature was found to have a marked effect on G/E, in that the curved panel had a larger value of G/E for the same τ.

Contour maps of τ, the shearing stress, have been constructed for the three panels.

II Acknowledgments

The authors wish to thank Dr. Theodore von Kármán, director of the Guggenheim Aeronautical Laboratory of the California Institute of Technology, for his advice and aid in treating the theoretical investigation. They also wish to thank Dr. E. E. Sechler, under whose direction the research was carried out, for his valuable assistance at all times; and W. L. Howland for his helpful suggestions.

Acknowledgment is also due L. G. Dunn for starting the investigation and for his aid throughout, and to the Lockheed Aircraft Company for the test specimens.

III. Introduction

The work covered by this paper is an extension of the work of White and Antz, who investigated reinforced flat plates under concentrated end loads, and the work of Lovett and Rodee, who investigated the transfer of stress from main beams to intermediate stiffeners, as a part of the investigation of stress distribution in metal covered wing leading to the most efficient distribution of materials. The authors have taken the case of two built up beam sections, connected by a Dural sheet reenforced with corrugation, and subjected to uniform bending moment. The transfer of compressive stress from the main spars to the corrugations through shear has been studied in order to find a suitable method of calculating the load in the corrugations.

Three combinations were tested, one of .040" plane sheet, one of .040" curved sheet, and one of .025" flat sheet, all with corrugation of thickness .032". The .040" sheets remained out of the wave state, at the max bending moment of 200,000 inch-pounds, but the .025" sheet buckled between rivet rows. The corrugation size and arrangement were the same on the three panels.

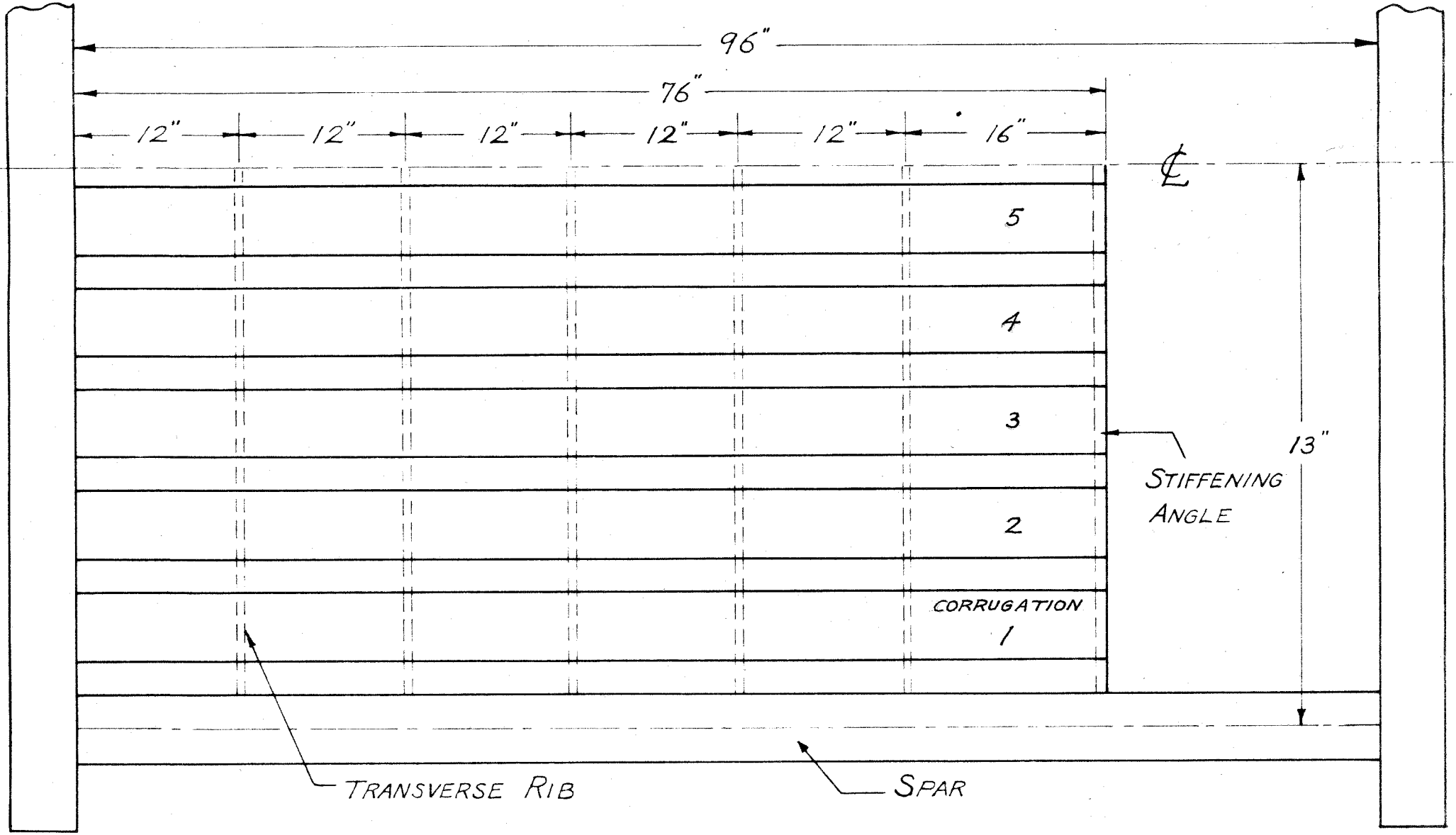

PLAN VIEW OF PANEL FIG. 1

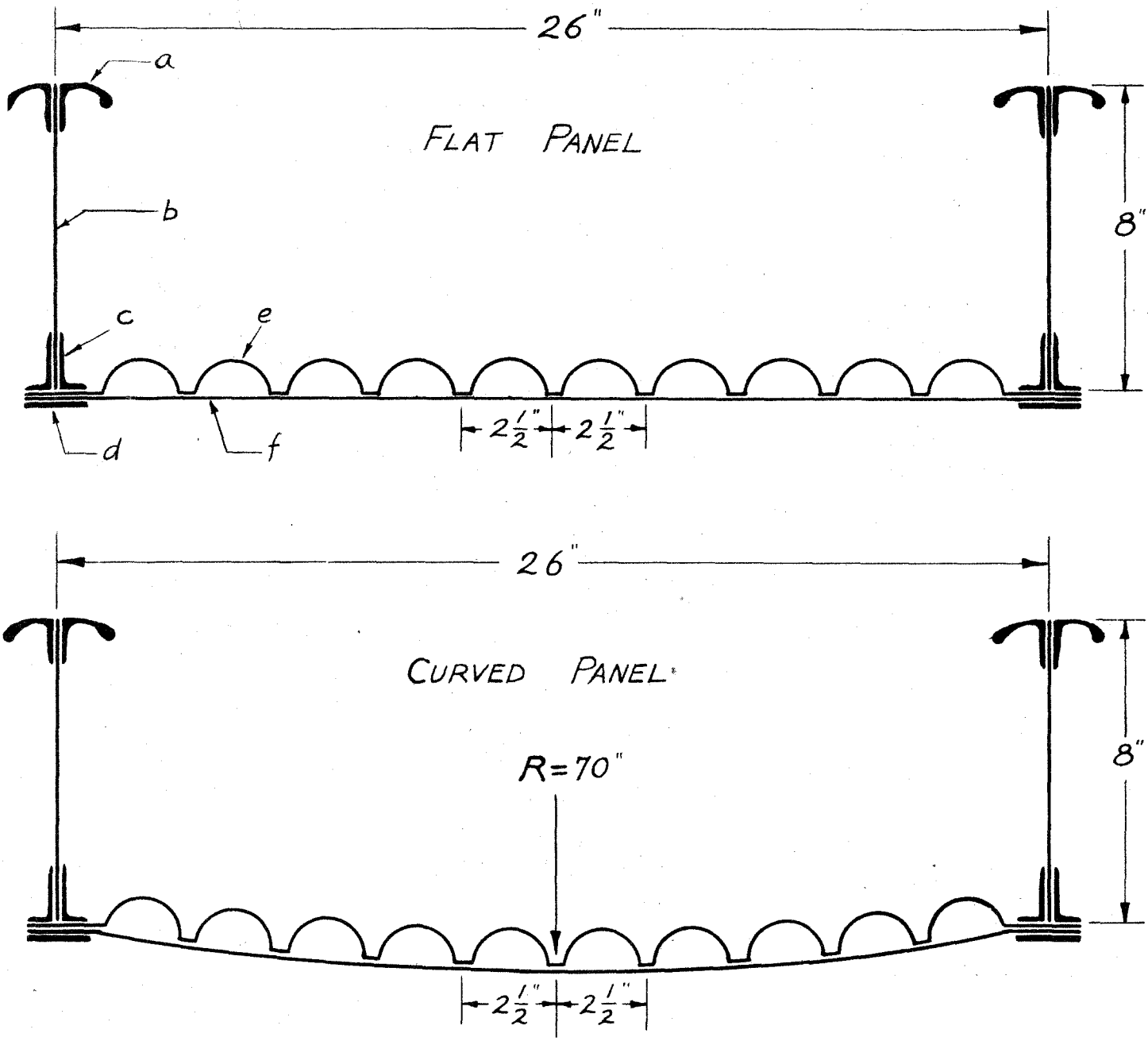

a. UPPER CAP ANGLE. AREA = 0.354 in^2
b. BEAM WEB. $t = 0.051$ in.
c. LOWER CAP ANGLE. AREA = 0.221 in^2
d. BOTTOM STRIP. AREA = 0.188 in^2
e. CORRUGATION. $t = 0.032$ in. $h = 0.844$ in.
f. COVER SHEET. $t_1 = 0.040$ in. $t_2 = 0.025$ in.

CROSS SECTION OF PANELS

FIG. 2

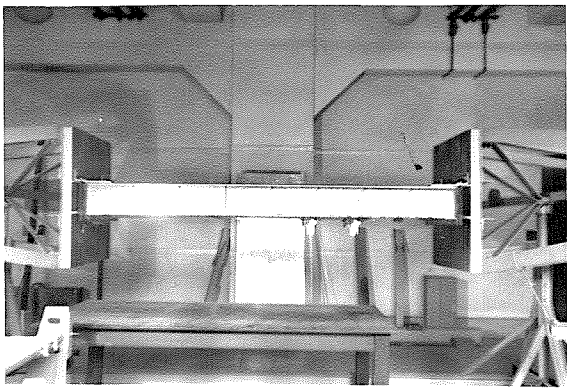

SIDE VIEW

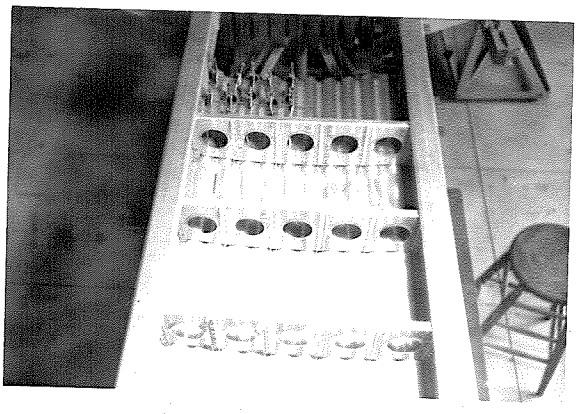

TOP VIEW

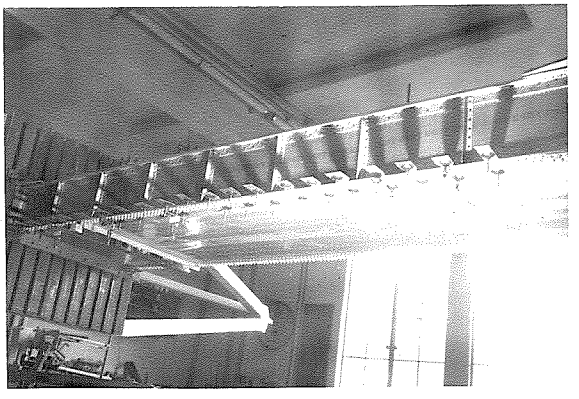

BOTTOM VIEW

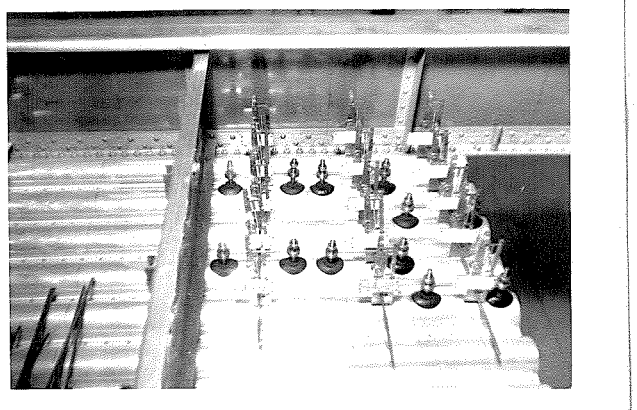

EXTENSOMETERS ON CORRUGATION TOP

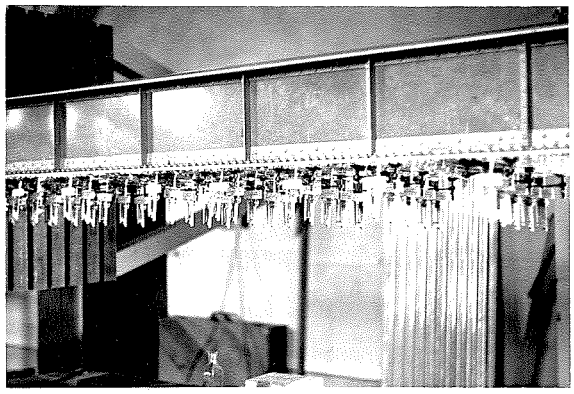

EXTENSOMETERS ON THE SKIN

IV. Experimental Investigation

The test specimen consisted of two main spars, 96 inches long and spaced 26 inches apart, and a bottom cover sheet of skin and corrugations 26 inches by 76 inches secured to the flange angles by two rows of 8/32 bolts spaced 3/4 of an inch apart. The corrugations were formed from flat sheet by using a male and female die in a 700 ton hydraulic brake, and have the shape of a Greek Capital letter Omega. There were ten corrugations between the spars, each corrugation being $2\frac{1}{2}$ inches wide. A row of 1/8 rivets spaced 1" apart between corrugations fastened them to the skin.

Both ends of the spar and one end of the cover sheet were rigidly attached to the testing machine and the other end of the cover sheet was free, but with a 1" x 1" x 3/32" angle riveted to the edge, and fastened to the spars.

At 1 ft. intervals along the span, chordwise, ribs were used to prevent the rotation of the spars. For a description of the testing machine and methods of loading see Ref. 1. The stress distribution was obtained by measuring deformations with Huggenberger type extensometers placed on the beam caps, on top of the corrugations, and on the skin directly below the maximum height of the corrugation. The extensometer gauge length used was two centimeters. For the .025" skin, which was in the wave state during loading, the latter readings were taken in the trough between corrugations and extropolated to the desired position.

The beam stress was first measured at the center of the bottom beam cap, and resulted in a curve as shown in Fig. 3, 4, and 5. The shape

of these curves agreeing closely with that of Lovett and Rodee. However, this beam curve does not satisfy our assumption that at any station the beam and corrugations must be in equilibrium, i.e. that between any two stations along the span, the load dropped by the beam must be taken up in Compression due to shear in the corrugations and sheet. Therefore, as a check, the stress at the outside edges of the bottom beam Cap was measured and plotted in Fig. 6. This plot definitely shows the presence of Chordwise bending. This check was made on the curved panel, after removal of the flat panel and therefore we were only able to correct the beam curve for the former, by taking an average of the stresses at the edges. This plot, Fig. 7, checked our assumption within .8 of 1 per cent.

Extensometer readings were taken for loads of 40, 80, 120, 160, and 200 Thousand inch-pounds, but the stresses were calculated only for the 200 thousand in.-pounds case, the other four readings being used for a stress-strain curve check on the validity of the 200 thousand reading. In converting strain into stress, the value of Young's Modulus for Duralumin was taken as 10×10^6 #/ Sq.in. Figs. 8 to 17 show typical stress distribution curves as obtained from the .040" flat panel.

Having now measured the stresses, it is necessary to eliminate the stresses due to the bending of each corrugation about some lateral axis. This has been done in the following manner:

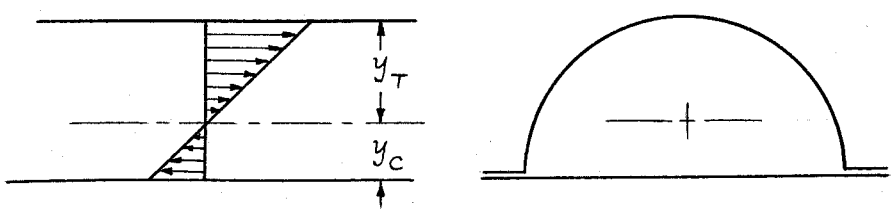

$\frac{MY_t}{I} = T_b$ (Tension due to bending)

$\frac{MY_c}{I} = C_b$ (Compression due to bending)

Since $\frac{M}{I}$ is the same for both:

$$\frac{T_b}{Y_t} = \frac{C_b}{Y_c}$$

or $$C_b = \frac{Y_c}{Y_t} T_b \quad -- \underline{1}.$$

Let $C_{s.h.}$ be the Compressive stress due to shear,
S_t. be the measured stress in the top of the Corrugation
S_b be the measured stress in the bottom of the Corrugation

$$S_t = C_{sh} - T_b \quad -- \underline{2}.$$

$$S_b = C_{sh} + C_b \quad -- \underline{3}.$$

Substituting 1 in 3 and multiplying 2 by $\frac{Y_c}{Y_t}$ gives:

$$\frac{Y_c}{Y_t} S_t = \frac{Y_c}{Y_t} C_{sh} - \frac{Y_c}{Y_t} T_b$$

$$S_b = C_{sh} + \frac{Y_c}{Y_t} T_b$$

Adding we obtain:

$$\frac{Y_c}{Y_t} S_t + S_b = \left(\frac{Y_c}{Y_t} + 1 \right) C_{sh}$$

$$\therefore \quad C_{sh} = \frac{\frac{Y_c}{Y_t} S_t + S_b}{1 + \frac{Y_c}{Y_t}}$$

Similarly for the case of the corrugation bending about a point outside of itself we obtain:

$$C_{sh} = \frac{\frac{Y_c}{Y_t} S_t - S_b}{-1 + \frac{Y_c}{Y_t}}$$

$\frac{Y_c}{Y_t}$ must be determined for each corrugation in order to calculate from the above equation. The exact position of the points about which the corrugations bend is unknown and the authors worked for some time attempting to determine them analytically and experimentally. However, it was found to be impossible to separate the measured stress into its component parts of stress due to shear, and stress due to bending. Without knowing the stress due to bending, the exact location of the point of bending cannot be found. Therefore, it was necessary to arbitarily assume the position of these points. The point in the beam web where the transverse theoretical neutral axis line terminates was measured by taking stress readings at the top cap and bottom cap of the beam.

See Fig. 18.

Furthermore, from physical considerations, we know that the shear value diminishes from some finite value at the spar to zero at the center line of the panel due to symetry. Therefore, any assumption of a neutral axis which does not show a diminishing compressive stress due to shear must be in error. Also our values of compressive stress due to shear must satisfy our assumption that the corrugations and sheet pick up all the load dropped by the beam. Thus we limit our assumptions to a certain degree.

Several assumptions, which were obviously wrong, were made to obtain the resultant variation of stress, and the final assumption that each corrugation bends about its own center of gravity gives by far the best results.

These assumptions are shown in Fig. 19 to 22.

It is seen that the usual assumption of a straight neutral axis across the width and through the center of gravity of the system is decidedly in error.

From the consideration of these curves and a check on our equilibrium condition, it was decided that the assumption of each corrugation bending out its on c. g. should be used.

Therefore the compressive stress due to shear was calculated on this basis and results in the curves as shown in Fig. 23 to 27.

V. Theoretical Calculations

Effective Shear Modulus.

An attempt has been made to calculate an effective shear modulus for the benefit of the designer who desires to know how to handle the stresses in a system of corrugations.

Using the strip theory, we will consider each corrugation as a block of material with an effective thickness, rigidly attached to the adjacent corrugations as shown in Fig. A.

Consider an element of width dx as shown and the indicated shearing forces $V_{.1}$ $V_{.2}$ etc.

The shearing force $V_1 = A_b$

Where A_b = area of the beam effective in compression.
A_c = area of the corrugation.

$$V_1 - V_2 = A_c \frac{\partial \sigma_{x_1}}{\partial x}$$
$$V_2 - V_3 = A_c \frac{\partial \sigma_{x_2}}{\partial x}$$
$$V_3 - V_4 = A_c \frac{\partial \sigma_{x_3}}{\partial x}$$
$$V_4 - V_5 = A_c \frac{\partial \sigma_{x_4}}{\partial x}$$
$$V_5 - V_6 = A_c \frac{\partial \sigma_{x_5}}{\partial x}$$

but $V_6 = 0$ from symetry.

$$\therefore V_5 = A_c \frac{\partial \sigma_{x_5}}{\partial x}$$

From this we may solve for each shearing force and find:

$$V_1 = A_c \left(\frac{\partial \sigma_{x_1}}{\partial x} + \frac{\partial \sigma_{x_2}}{\partial x} + \frac{\partial \sigma_{x_3}}{\partial x} + \frac{\partial \sigma_{x_4}}{\partial x} + \frac{\partial \sigma_{x_5}}{\partial x} \right)$$
$$V_2 = A_c \left(\frac{\partial \sigma_{x_2}}{\partial x} + \frac{\partial \sigma_{x_3}}{\partial x} + \frac{\partial \sigma_{x_4}}{\partial x} + \frac{\partial \sigma_{x_5}}{\partial x} \right)$$

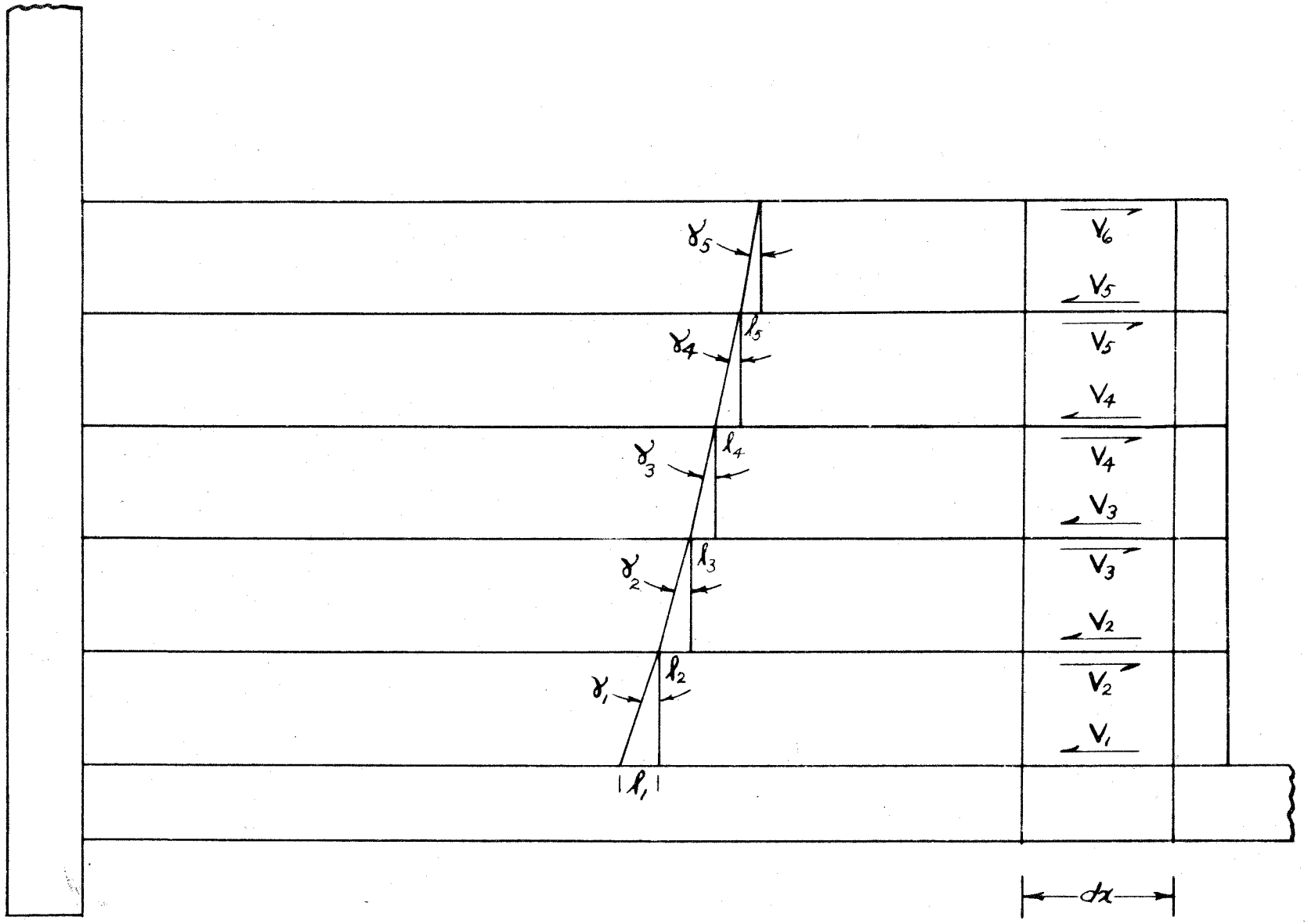
γ_5
γ_4
γ_3
γ_2
γ_1
ℓ_5
ℓ_4
ℓ_3
ℓ_2
ℓ_1
V_6
V_5
V_4
V_3
V_2
V_1
dx

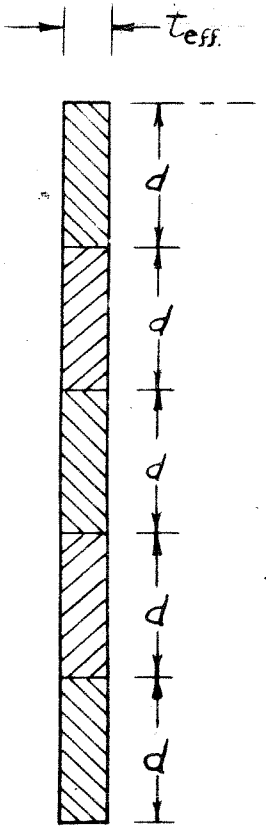
$t_{eff.}$
d
d
d
d
d

FIG. A

$$V_3 = A_c\left(\frac{\partial \sigma_{x3}}{\partial x} + \frac{\partial \sigma_{x4}}{\partial x} + \frac{\partial \sigma_{x5}}{\partial x}\right)$$
$$V_4 = A_c\left(\frac{\partial \sigma_{x4}}{\partial x} + \frac{\partial \sigma_{x5}}{\partial x}\right)$$
$$V_5 = A_c\left(\frac{\partial \sigma_{x5}}{\partial x}\right)$$
$$V_6 = 0$$

Also the basic relationship between the shearing stress τ and the strain angle γ is: $\tau = G\gamma$ where G = Shear modulus.

Therefore for corrugation 1:

$$\frac{V_1 + V_2 = \tau_1}{2t} = G_1 \gamma_1$$

for 2 $$\frac{V_2 + V_3}{2t} = G_2 \gamma_2$$

$$\frac{V_3 + V_4}{2t} = G_3 \gamma_3 \qquad \text{and etc.}$$

" "

$$\frac{V_5}{2t} = G_5 \gamma_5 \qquad \text{since } V_6 = 0$$

$$\therefore G_1 = \frac{V_1 + V_2}{2t\,\gamma_1} = \frac{A_c\left[\frac{\partial \sigma_{x1}}{\partial x} + 2\frac{\partial \sigma_{x2}}{\partial x} + 2\frac{\partial \sigma_{x3}}{\partial x} + 2\frac{\partial \sigma_{x4}}{\partial x} + 2\frac{\partial \sigma_{x5}}{\partial x}\right]}{2t\,\gamma_1}$$

We may write:

$$\gamma_1 = \frac{\ell_1}{d} \qquad \text{for small angles,}$$

Where d is the corrugation width and ℓ_1 is the shortening of corrugation 1 relative to corrugation 2 and must be found at the point of contact between the spar and the first effective block in this case. Similarly ℓ_2 is the shortening of corrugation 2 and must be found at the point of contact of block 1 and 2. However due to the impractibility of measuring stresses at the rivet line, our stresses have been measured at the center of the corrugation. By graphically integrating between stresses curves σ_1 and σ_2 (say), to any station n (as shown in Fig. B)

we obtain the shortening of corrugation 2 relative to corrugation 3 the center of the corrugation and etc., since

$$\ell_{c_2} = \frac{1}{E}\left[\text{AREA UNDER } \sigma_1 \text{ CURVE} - \text{AREA UNDER } \sigma_2 \text{ CURVE}\right]$$

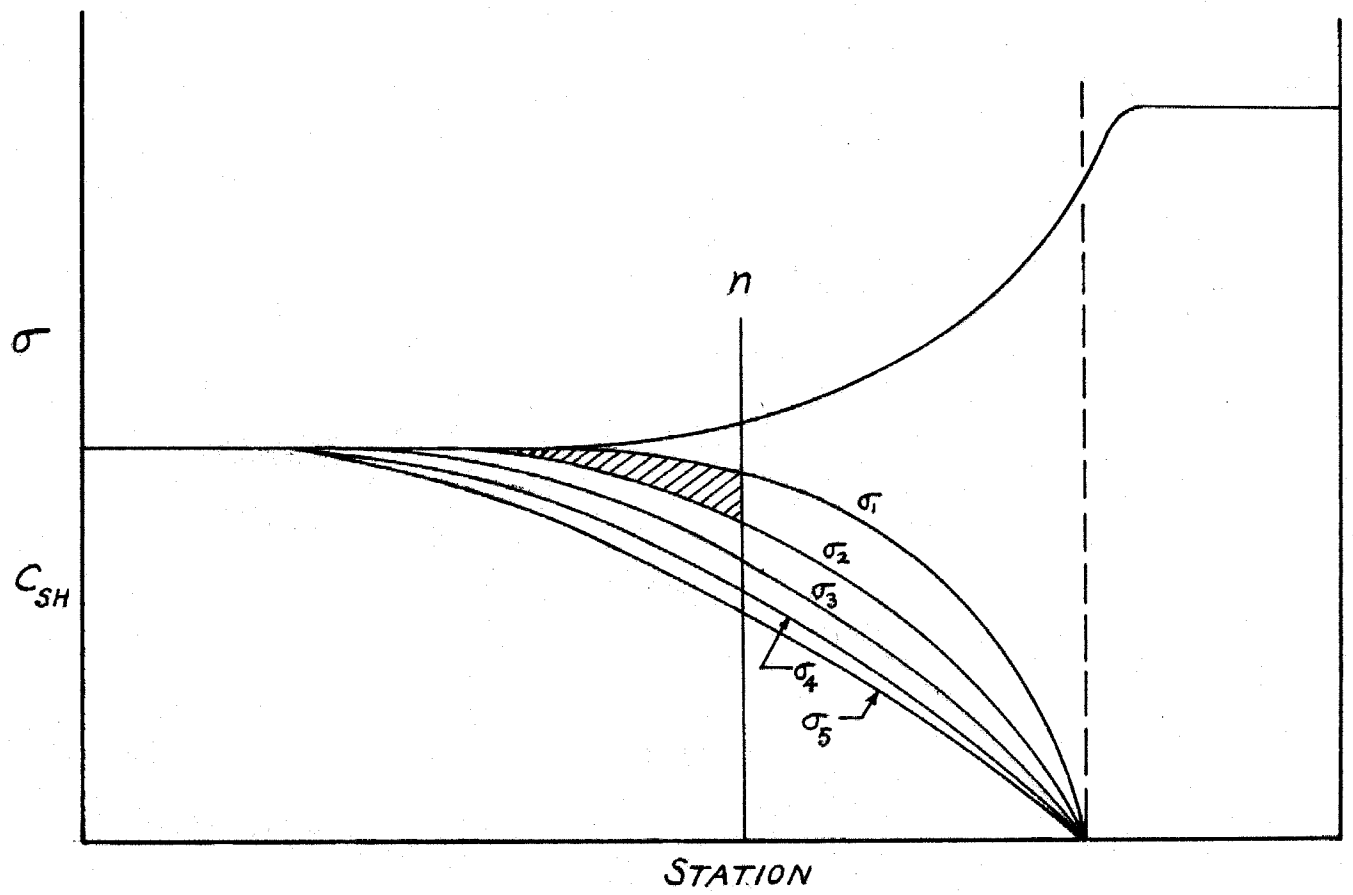

$$\ell_{c_2} = \frac{1}{E}\left[\text{AREA UNDER } \sigma_1 \text{ CURVE} - \text{AREA UNDER } \sigma_2 \text{ CURVE}\right]$$

RELATIVE SHORTENING OF CORRUGATIONS

FIG. B

Therefore in order to obtain the shortening of these blocks at the point of contact, we plot the integrated areas versus panel width and interpolate our desired area.

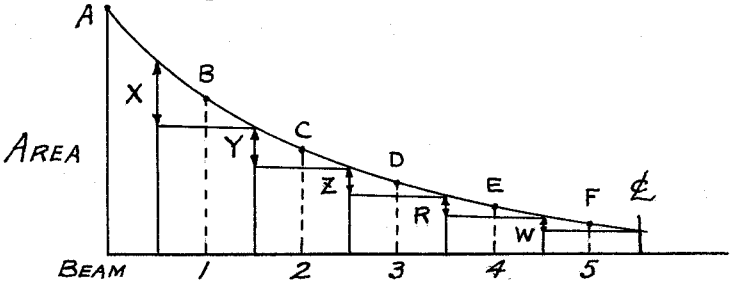

FIG. D

A, B, C, etc., are the integrated areas under the stress curves σ_B, σ_1, σ_2, *etc.* respectively.

Midway on the curve between A and B, for instance, is a point corresponding to the area under a stress curve if the stress were measured at the joint between block one and the beam. Similarly a point midway between B and C is the area under a stress curve measured at connection between block 2 and 3. Therefore X, as shown, is the difference between these two areas, or the shortening of block 1 relative to block 2. SIMILARLY Y, Z, R & W CAN BE OBTAINED FOR THE OTHER BLOCKS.

$$\therefore \quad \ell_2 = \frac{1}{E}\left[Y \right]$$

$$\therefore \quad \frac{G_1}{E} = \frac{A_c\left[\frac{\partial \sigma_{x1}}{\partial x} + 2\frac{\partial \sigma_{x2}}{\partial x} + 2\frac{\partial \sigma_{x3}}{\partial x} + 2\frac{\partial \sigma_{x4}}{\partial x} + 2\frac{\partial \sigma_{x5}}{\partial x}\right]}{\frac{2t}{d}\left[X\right]}$$

$$\frac{G_2}{E} = \frac{A_c\left[\frac{\partial \sigma_{x2}}{\partial x} + 2\frac{\partial \sigma_{x3}}{\partial x} + 2\frac{\partial \sigma_{x4}}{\partial x} + 2\frac{\partial \sigma_{x5}}{\partial x}\right]}{\frac{2t}{d}\left[Y\right]}$$

$$\frac{G_3}{E} = \frac{A_c\left[\frac{\partial \sigma_{x3}}{\partial x} + 2\frac{\partial \sigma_{x4}}{\partial x} + 2\frac{\partial \sigma_{x5}}{\partial x}\right]}{\frac{2t}{d}\left[Z\right]}$$

$$\frac{G_4}{E} = \frac{A_c\left[\frac{\partial \sigma_{x4}}{\partial x} + 2\frac{\partial \sigma_{x5}}{\partial x}\right]}{\frac{2t}{d}[R]}$$

$$\frac{G_5}{E} = \frac{A_c\left[\frac{\partial \sigma_{x5}}{\partial x}\right]}{\frac{2t}{d}[W]}$$

WHERE t = EFFECTIVE THICKNESS OF THE BLOCK.

The results of these formulae were plotted in Figs. and were, for a time, hard to explain, since the effective shear modulus obtained for corrugation 5 was less than that for corrugation 1, although the shearing stress in corrugation 1 was the greater. Normally one would expect a lower value of G/E for a higher value of τ. Span-wise the trend was correct with a higher effective shear modulus for a lower value of τ.

At the suggestion of Dr. von Karman, the chord-wise deformation in the panel, ε_y, was measured and plotted in Fig. Thus it is found that the measured γ differs from the actual γ and the corrections shown in Fig. must be applied.

The corrected results are plotted in Fig

——— CORRECT
– – – – – – MEASURED

(a) PURE COMPRESSION

$$\gamma = \gamma_m - \Delta\gamma$$

γ = CORRECT γ

γ_m = MEASURED γ

$\Delta\gamma$ = AMOUNT OF CORRECTION

$$= \frac{\partial \varepsilon_x}{\partial y}$$

$\varepsilon_x \ll \varepsilon_y$, SINCE $\Delta\gamma$ IS SMALL.

HENCE $\Delta\gamma$ IS NEGLIGIBLE COMPARED TO γ_m.

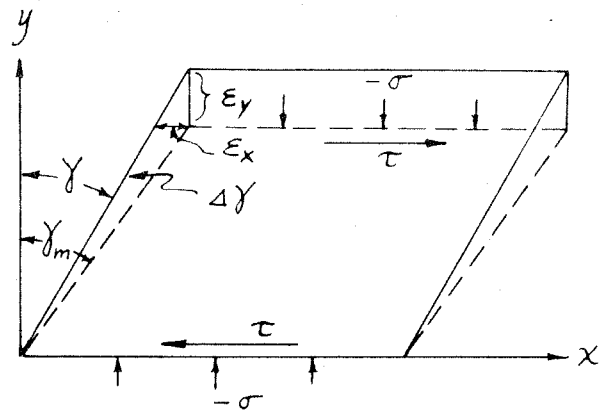

(b) PURE TENSION

$$\gamma = \gamma_m + \Delta\gamma$$

$\Delta\gamma$ IS ALSO NEGLIGIBLE

$$\Delta\gamma = \frac{\partial \varepsilon_x}{\partial y}$$

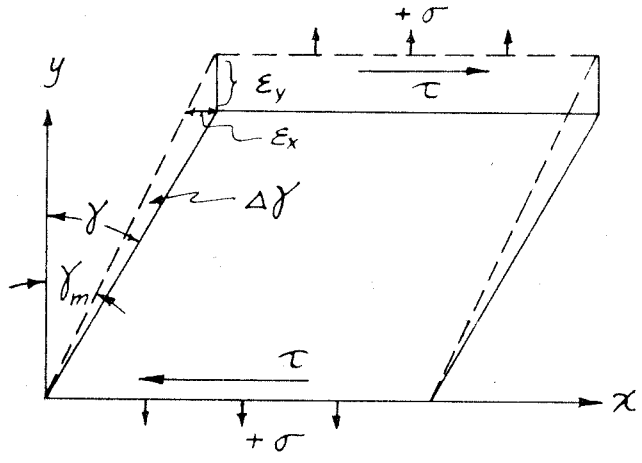

(c) COMPRESSION DUE TO BENDING BY SHEAR

$$\gamma = \gamma_m - \Delta\gamma$$

$$\Delta\gamma = \frac{\partial \varepsilon_y}{\partial x}$$

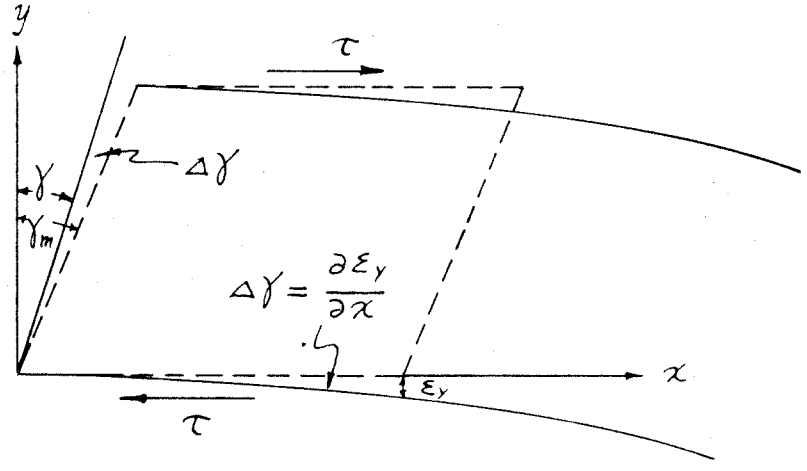

(d) TENSION DUE TO BENDING BY SHEAR

$$\gamma = \gamma_m + \Delta\gamma$$

$$\Delta\gamma = \frac{\partial \varepsilon_y}{\partial x}$$

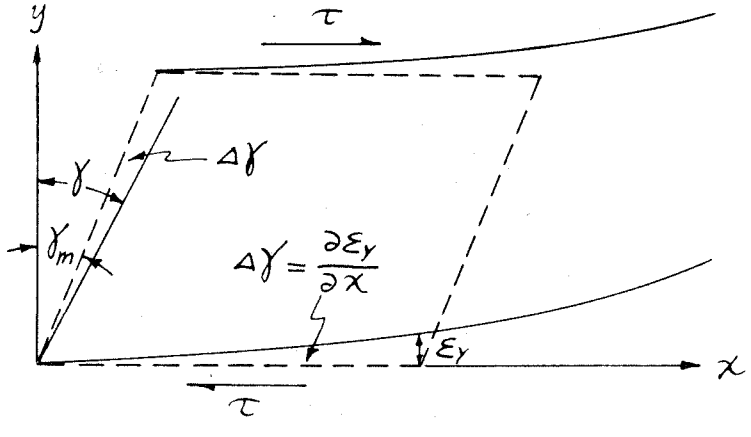

EFFECT OF CHORDWISE DEFORMATION ON UNIT SHEARING STRAIN, γ

FIG. C

to obtain t:

$$t_e = t_s + t_c \frac{l_c}{l_s}$$

Where t_c = corrugation thickness

t_s = skin "

l_c = length of corrug.

l_s = length of skin.

$\therefore$ t_e = .081" for .040" skin and .032" corrug.

t_e = .0667 for .025" skin and .032" corrug.

d = 2.5 inches

A_c = .2045 □" FOR .040" SKIN

= .167 □" FOR .025" SKIN

The results of these formulae are plotted in Fig. to .

Sample Calculation of G/E.

By graphical methods we find the slope of the C_{sh} curve for corrugations 1 to 5 at station 60 for the .040" plane sheet , obtaiming:

$$\frac{\partial \sigma_{x1}}{\partial x} = 55\#/\text{in.}$$

$$\frac{\partial \sigma_{x2}}{\partial x} = 150 \text{ "}$$

$$\frac{\partial \sigma_{x3}}{\partial x} = 230 \text{ "}$$

$$\frac{\partial \sigma_{x4}}{\partial x} = 220 \text{ "}$$

$$\frac{\partial \sigma_{x5}}{\partial x} = 210 \text{ "}$$

$A_c = .2045 \square"$

$t = .081$ "

$d = 2.5"$

Area under the σ_B curve = 522,000 #/in.

" " " σ_1 " = 485,200 "

" " " σ_2 " = 468,400 "

" " " σ_3 " = 446,400 "

" " " σ_4 " = 424,200 "

" " " σ_5 " = 410,800 "

Plotting these areas versus the width of the panel, and and interpolating, as shown in Fig. D, we obtain:

X = 33000 #/in.

Y = 24000 "

Z = 21000 "

R = 18000 "

W = 12000 "

Therefore:

$$G'/E = \frac{.2045\ (\ 55 + 2\times150 + 2\times230 + 2\times220 + 2\times210\ )}{\frac{2\times.081}{2.5}\ (\ 33000)}$$

$G'/E = .161$ for station 60" (corrugation 1)

τ for the same station and corrugation is:

$$\tau_1 = \frac{V_1}{t}$$

$$V_1 = A_c\left[\frac{\partial \sigma_{x_1}}{\partial x} + \frac{\partial \sigma_{x_2}}{\partial x} + \cdots \frac{\partial \sigma_{x_5}}{\partial x}\right]$$

$V_1 = 177$ #/IN.

$t = .081$ "

$$\tau = \frac{177}{.081} = 2190\ \#/\square"$$

Sample Calculation for correcting the measured value of G/E.

Curved panel - Corrugation 5 -- Station 72.5"

$$\Delta\gamma = \frac{\partial \varepsilon_y}{\partial x} = 1.80 \times 10^{-4}$$

$$\gamma_{MEASURED} = \frac{W}{d \cdot E} = \frac{5{,}000\ \#/in.}{2.5\ in\ \ 10^7\ \#/in^2} = 2.0 \times 10^{-4}$$

$$\gamma = \gamma_{MEASURED} - \Delta\gamma$$

$$= 2.0 \times 10^{-4} - 1.80 \times 10^{-4} = 0.20 \times 10^{-4}$$

$$\left(\frac{G'}{E}\right)_{ACTUAL} = \left(\frac{G'}{E}\right)_{MEASURED} \cdot \frac{1}{\frac{\gamma}{\gamma_m}}$$

$$= 0.0379 \cdot \frac{1}{\frac{.20 \times 10^{-4}}{2.0 \times 10^{-4}}}$$

$$= 0.379$$

VI Discussion of Results.

It is seen that the value of the effective shear modulus decreases from the spar to the center line unless take into account the chord-wise deformations, ε_y, because $\frac{\partial \varepsilon_y}{\partial x}$ has such a large effect on γ. Having applied the necessary correction, we obtain the expected result that the effective shear modulus, G'/E, decreases with increasing τ, and is, within experimental error, the same for each corrugation for one value of τ.

The test set-up had many eccentricities; chordwise bending was present, the stiffening angle across the free end of the panel affected the measurements, and in general, much scatter of the experimental points was the result.

For this system we have the two equilibrium equations:

$$\frac{\partial \sigma_x}{\partial x} + \frac{\partial \tau}{\partial y} = 0$$

$$\frac{\partial \tau}{\partial x} + \frac{\partial \sigma_y}{\partial y} = 0$$

We have neglected $\frac{\partial \sigma_y}{\partial y}$, and have justified it from the measurements of ε_y, these stresses indicating that the effects of $\frac{\partial \sigma_y}{\partial y}$ are negligible as well as inconsistent.

Contour maps of τ, the shearing stress, were constructed and shown in Figs. 28 to 30. These maps differ slightly from what one would expect, due to the effect of the stiffening angle on the free edge of the sheet. The .040" curved panel shows close agreement to what has been found in Photo-Elastic experiments.

The .040" curved panel appears to pick up its compressive stress due to shear faster than the other combinations.

Some results on corrugation and sheet combinations subjected to pure compression will be necessary before more accurate assumptions can be made regarding the compressive stress due to shear and the stresses due to bending in order to find the neutral axis of such a system.

References

1. Lovett, B. B. C, and Rodee, W. F. :
"The Transfer of Stress from main beams to intermediate stiffeners in metal Sheet Covered Box Beams." M. S. Thesis C. I. T. 1936 and Journal of Aeronautic Sciences Volume 3, No. 12, Page 426, October 1936.

2. White, R. J. and Antz, Hans M.:
The stress distribution in reenforced plates under concentrated end loads. M. S. Thesis C. I. T. 1935 and J. Ae. S. Volume 3, No. 6, Page 209, April 1936.

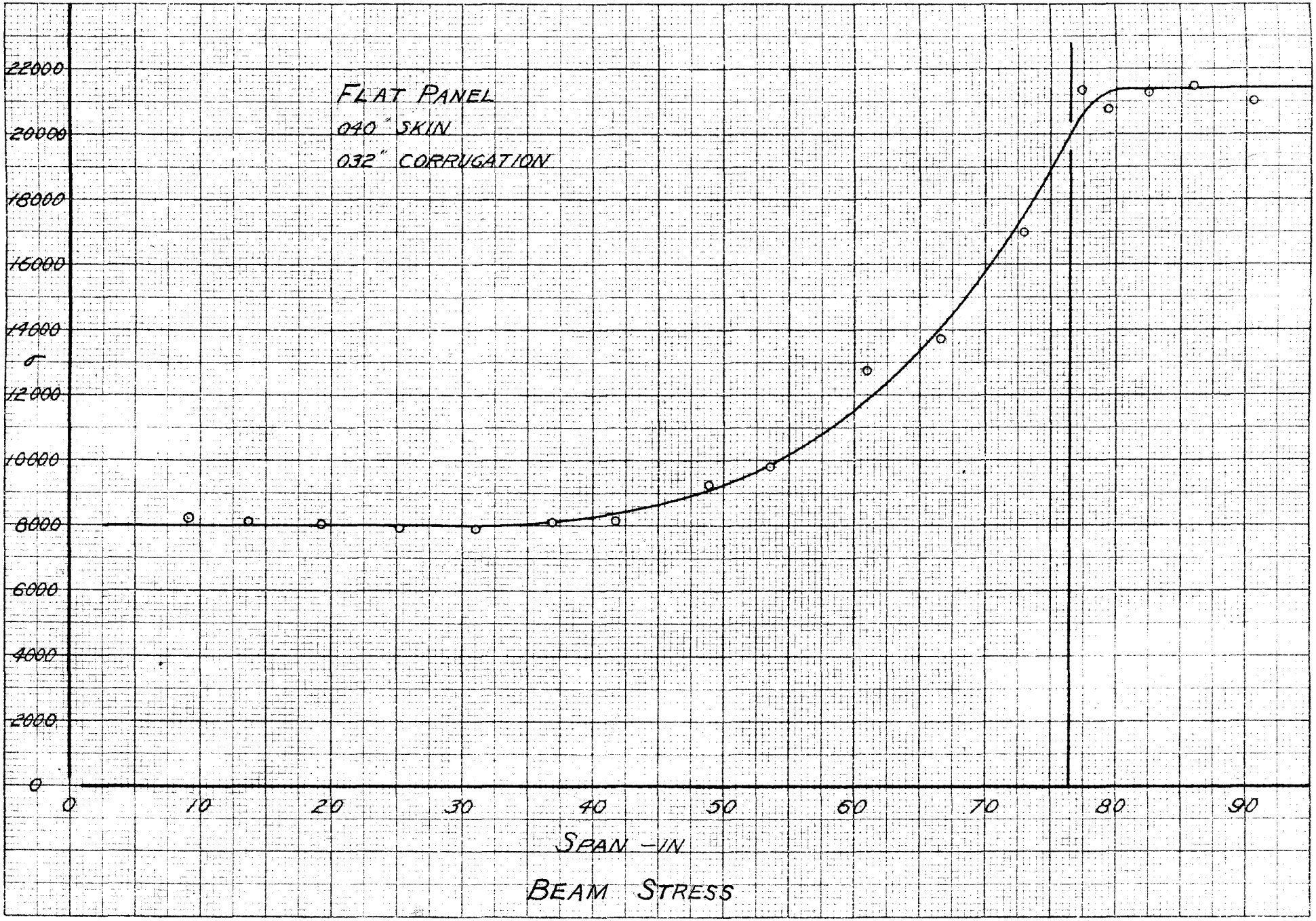
FLAT PANEL
.040" SKIN
.032" CORRUGATION
22000
20000
18000
16000
14000
σ
12000
10000
8000
6000
4000
2000
0
0
10
20
30
40
50
60
70
80
90
SPAN - IN
BEAM STRESS

FIG. 3

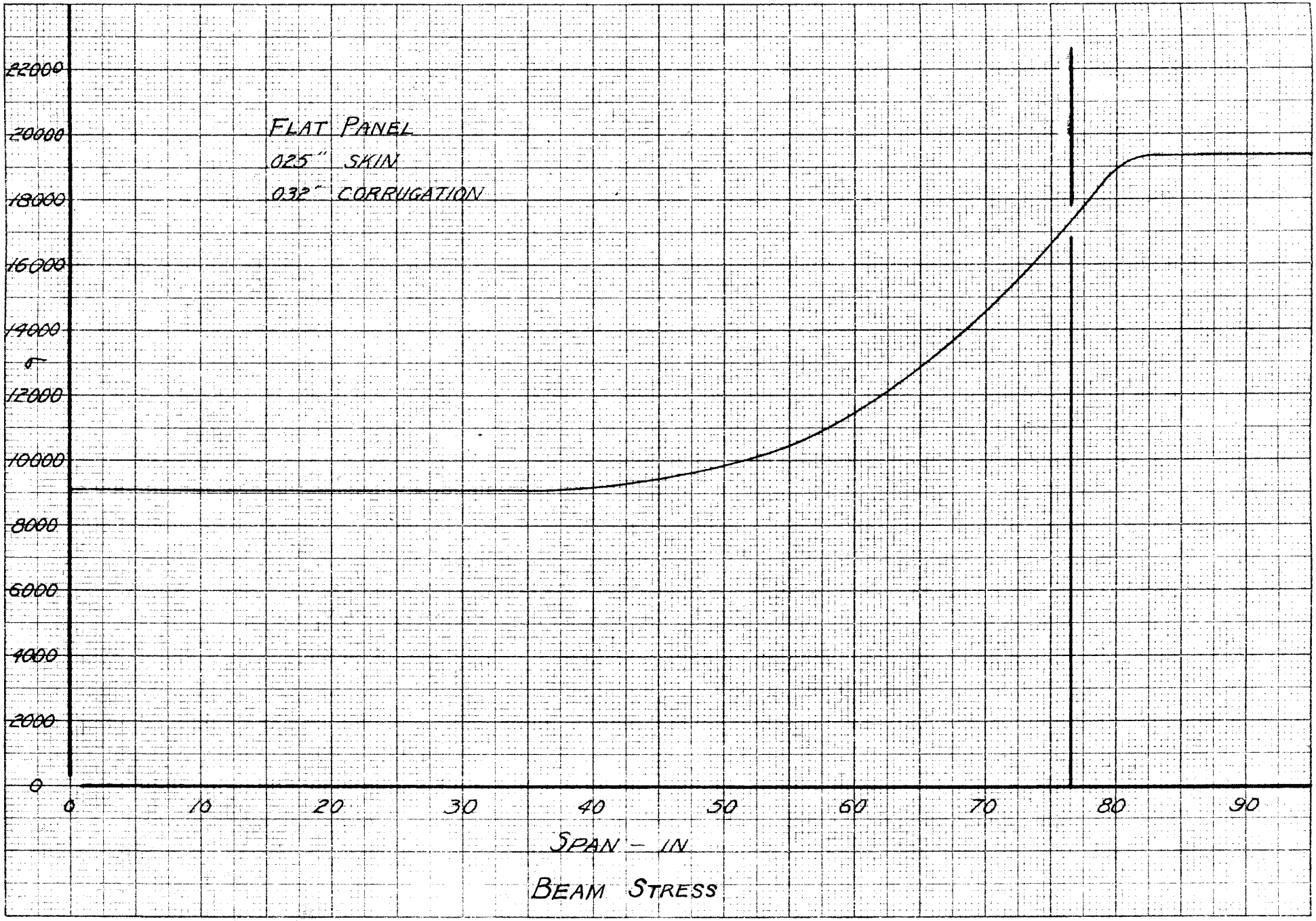
FLAT PANEL
.025" SKIN
.032" CORRUGATION
22000
20000
18000
16000
14000
12000
10000
8000
6000
4000
2000
0
0
10
20
30
40
50
60
70
80
90
SPAN - IN
BEAM STRESS

FIG. 4

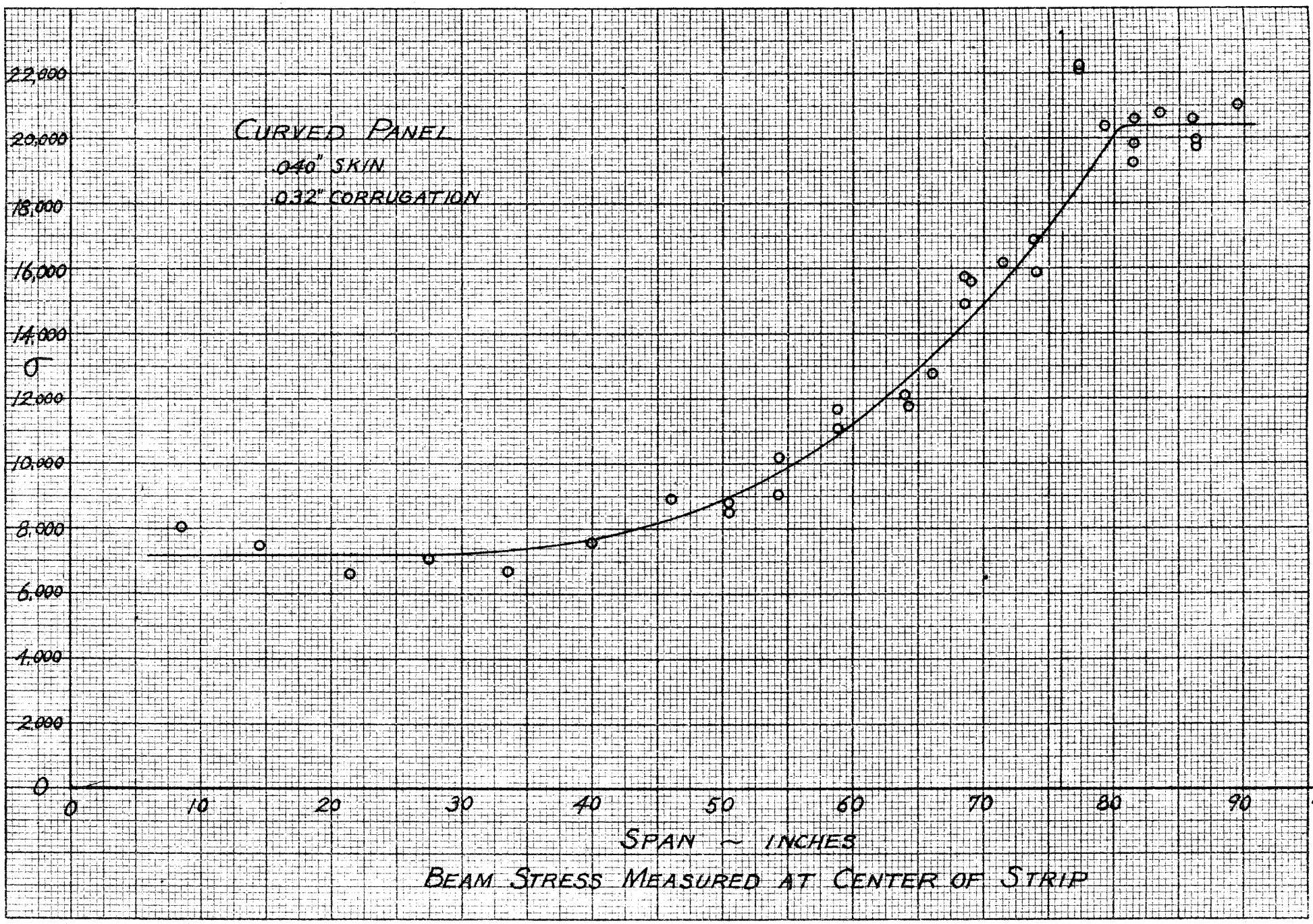
CURVED PANEL
.040" SKIN
.032" CORRUGATION
22,000
20,000
18,000
16,000
14,000
σ
12,000
10,000
8,000
6,000
4,000
2,000
0
0
10
20
30
40
50
60
70
80
90
96
SPAN ~ INCHES
BEAM STRESS MEASURED AT CENTER OF STRIP

FIG. 5.

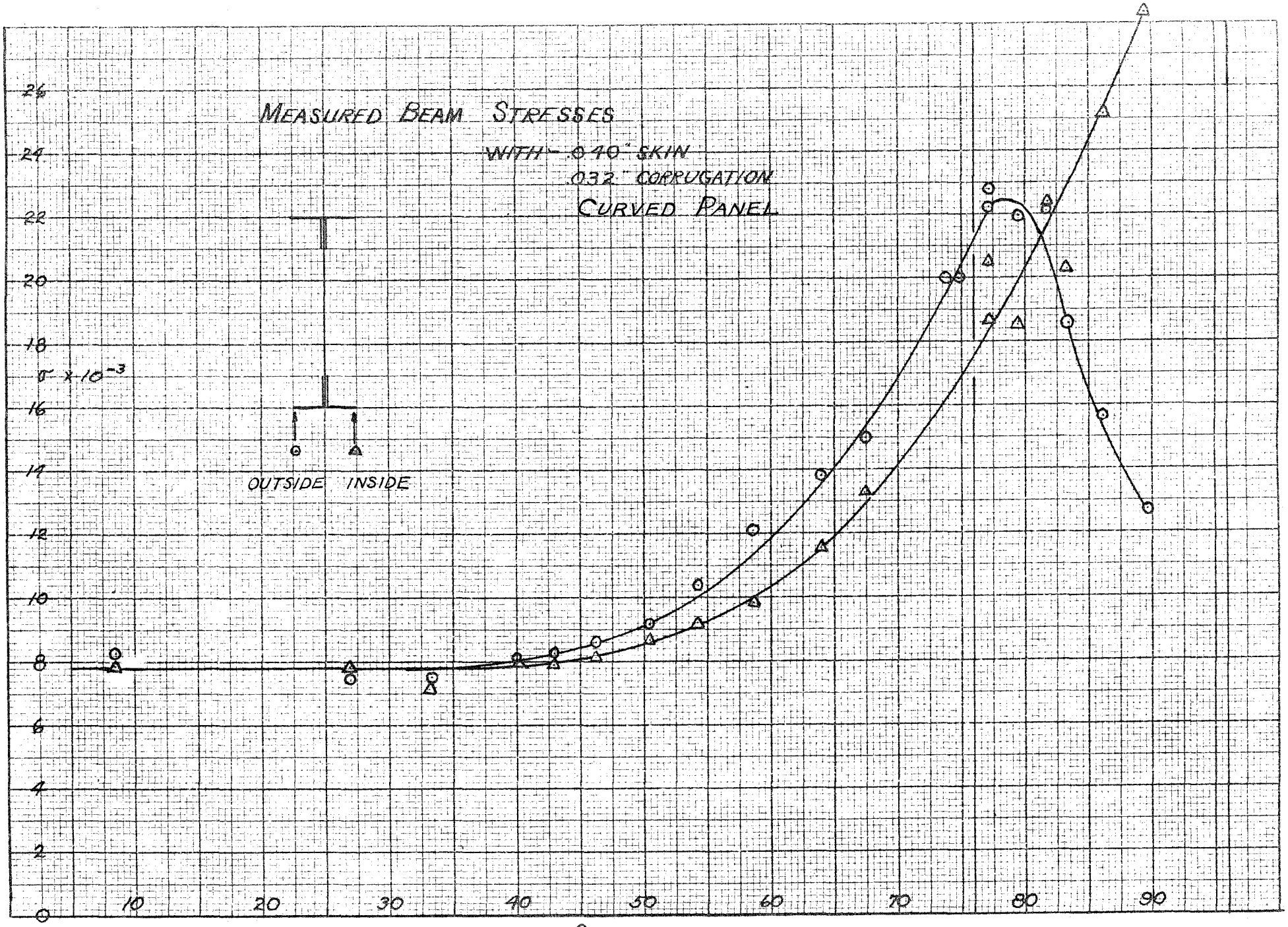
MEASURED BEAM STRESSES
WITH - .040" SKIN
.032" CORRUGATION
CURVED PANEL
σ x 10⁻³
OUTSIDE
INSIDE
SPAN - IN.
0
2
4
6
8
10
12
14
16
18
20
22
24
26
10
20
30
40
50
60
70
80
90

FIG. 6

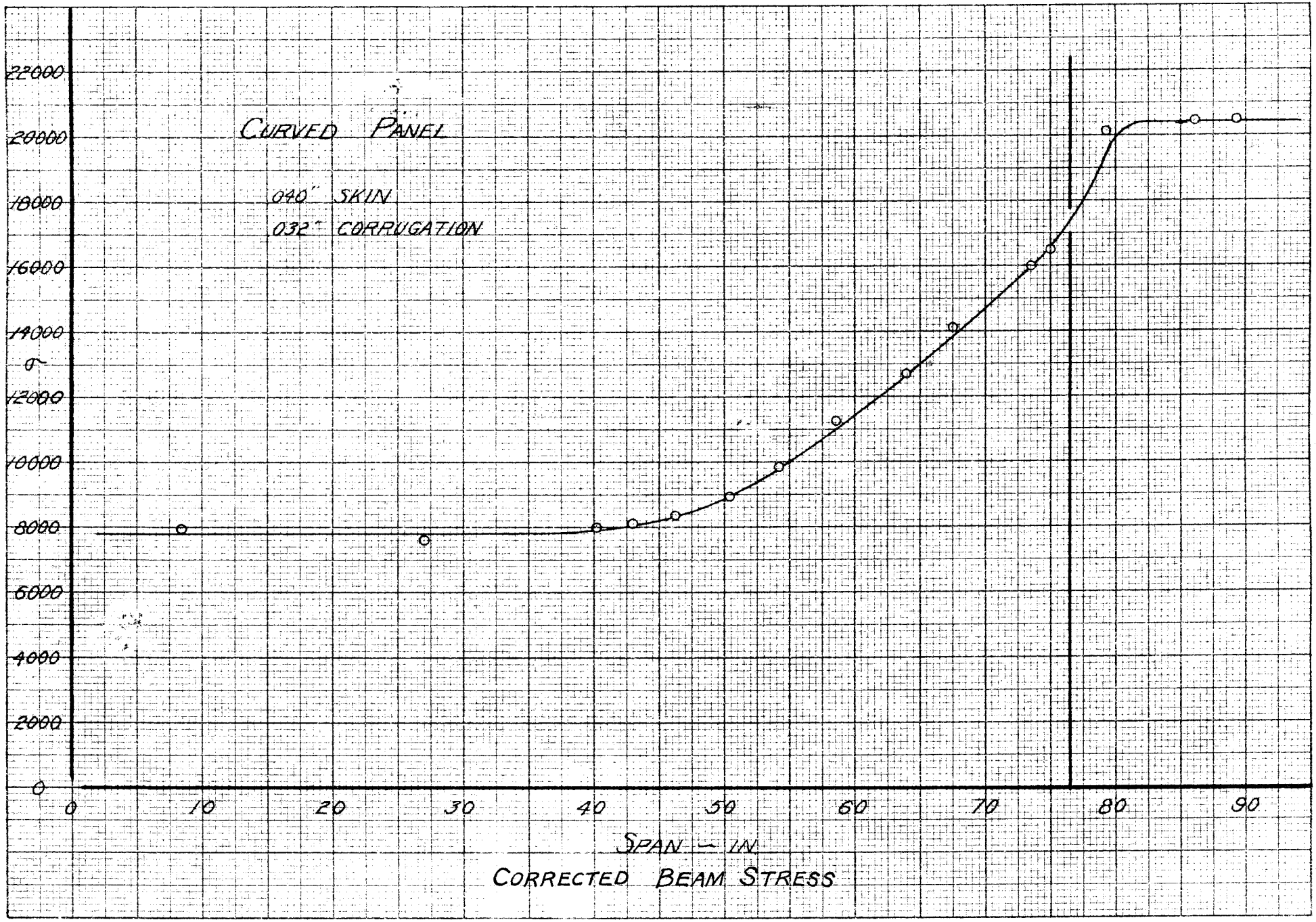
CURVED PANEL
.040" SKIN
.032" CORRUGATION
22000
20000
18000
16000
14000
12000
10000
8000
6000
4000
2000
0
0
10
20
30
40
50
60
70
80
90
SPAN — IN.
CORRECTED BEAM STRESS

FIG. 7

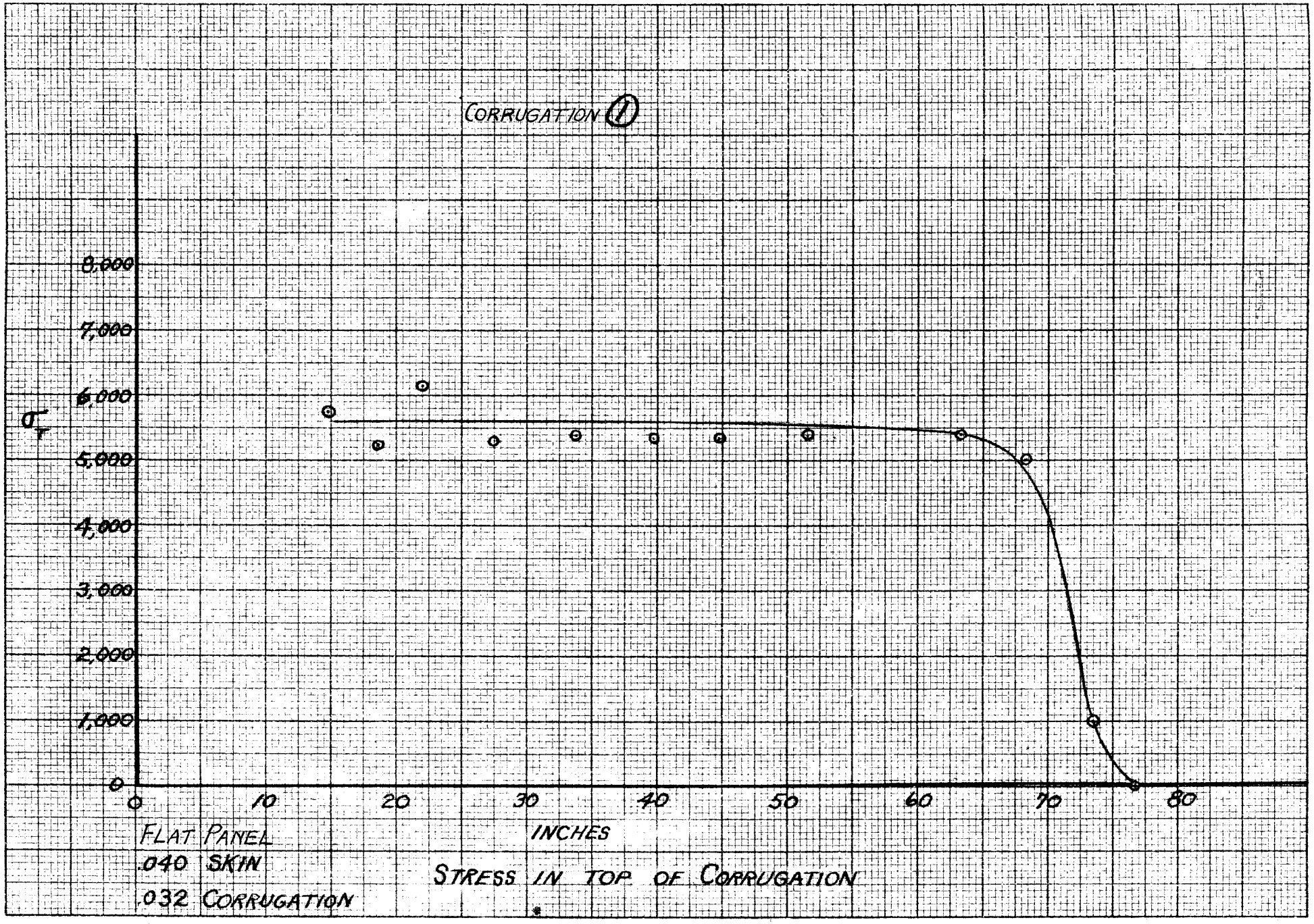
CORRUGATION (1)
8,000
7,000
6,000
5,000
4,000
3,000
2,000
1,000
0
σ_T
0
10
20
30
40
50
60
70
80
INCHES
FLAT PANEL
.040 SKIN
.032 CORRUGATION
STRESS IN TOP OF CORRUGATION

FIG. 8

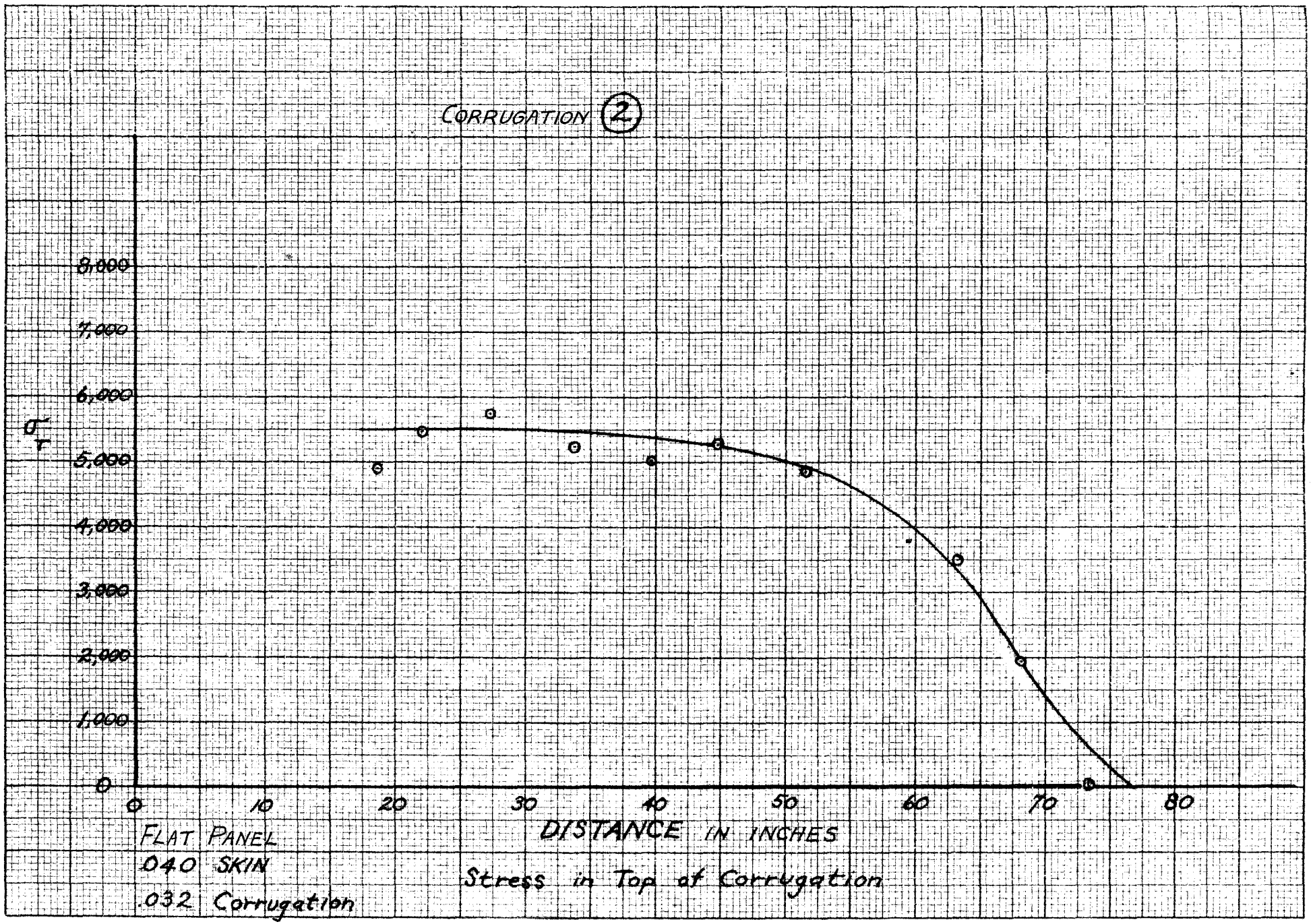
CORRUGATION (2)
8,000
7,000
6,000
σ_T
5,000
4,000
3,000
2,000
1,000
0
0
10
20
30
40
50
60
70
80
DISTANCE IN INCHES
FLAT PANEL
.040 SKIN
.032 Corrugation
Stress in Top of Corrugation

FIG. 9

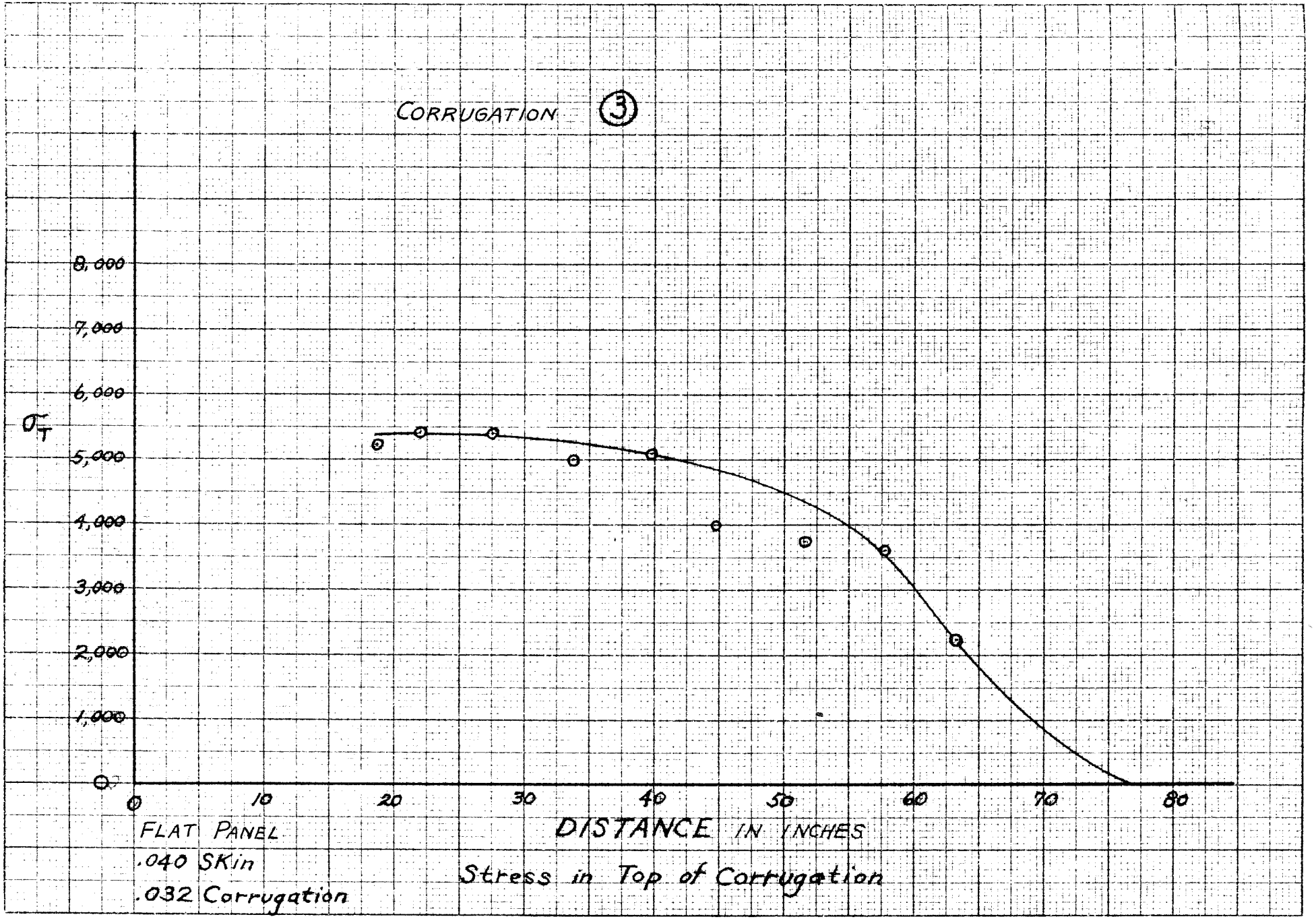
CORRUGATION (3)
8,000
7,000
6,000
σ_T
5,000
4,000
3,000
2,000
1,000
0
0
10
20
30
40
50
60
70
80
DISTANCE IN INCHES
FLAT PANEL
.040 SKin
.032 Corrugation
Stress in Top of Corrugation

FIG. 10

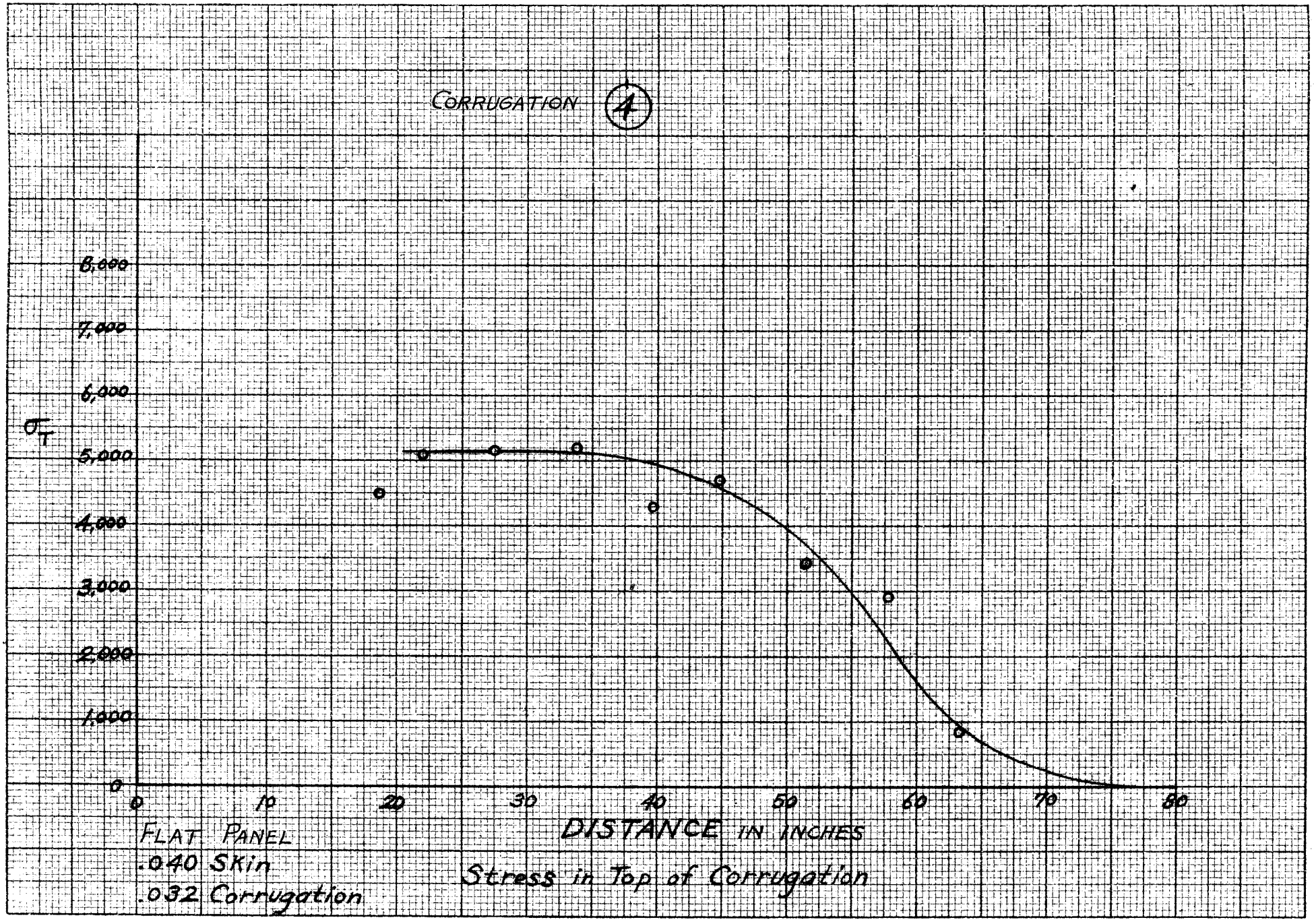
CORRUGATION 4
8,000
7,000
6,000
σ_T
5,000
4,000
3,000
2,000
1,000
0
0
10
20
30
40
50
60
70
80
DISTANCE IN INCHES
FLAT PANEL
.040 SKin
.032 Corrugation
Stress in Top of Corrugation

FIG. 11

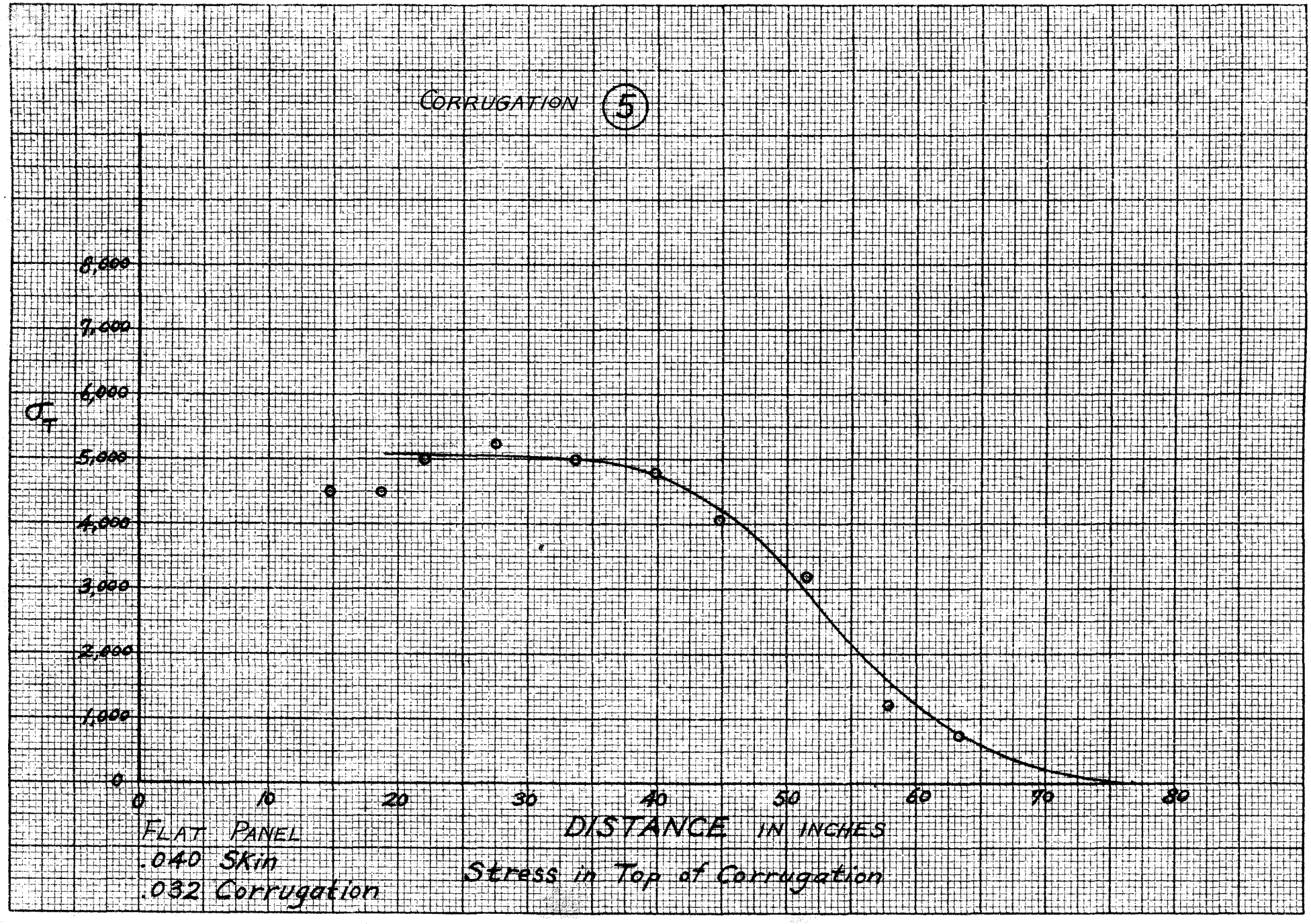
CORRUGATION (5)
8,000
7,000
6,000
σ_T
5,000
4,000
3,000
2,000
1,000
0
0
10
20
30
40
50
60
70
80
DISTANCE IN INCHES
FLAT PANEL
.040 Skin
.032 Corrugation
Stress in Top of Corrugation

FIG. 12

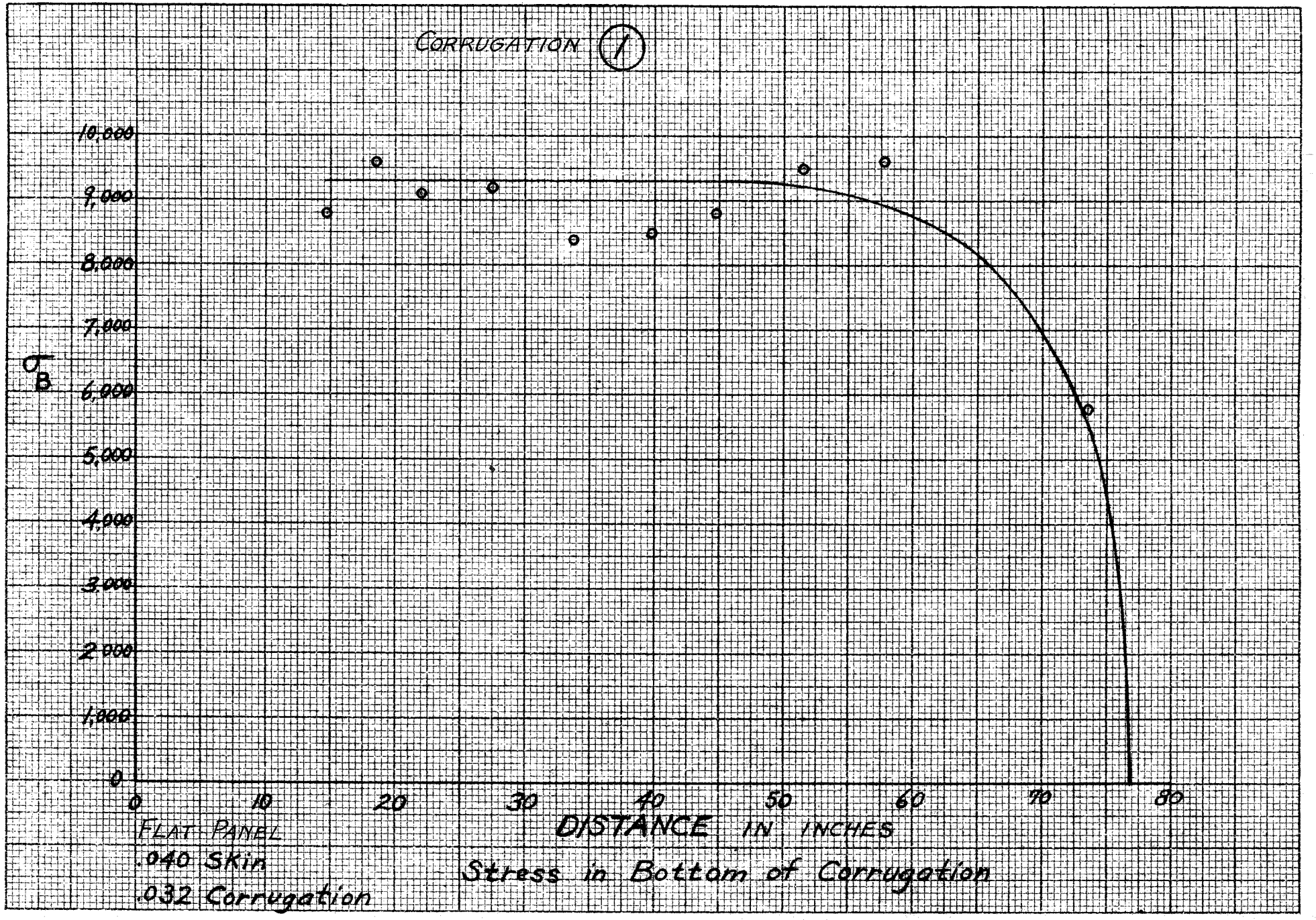
CORRUGATION (1)
10,000
9,000
8,000
7,000
σ_B
6,000
5,000
4,000
3,000
2,000
1,000
0
0
10
20
30
40
50
60
70
80
DISTANCE IN INCHES
FLAT PANEL
.040 SKin
.032 Corrugation
Stress in Bottom of Corrugation

FIG. 13

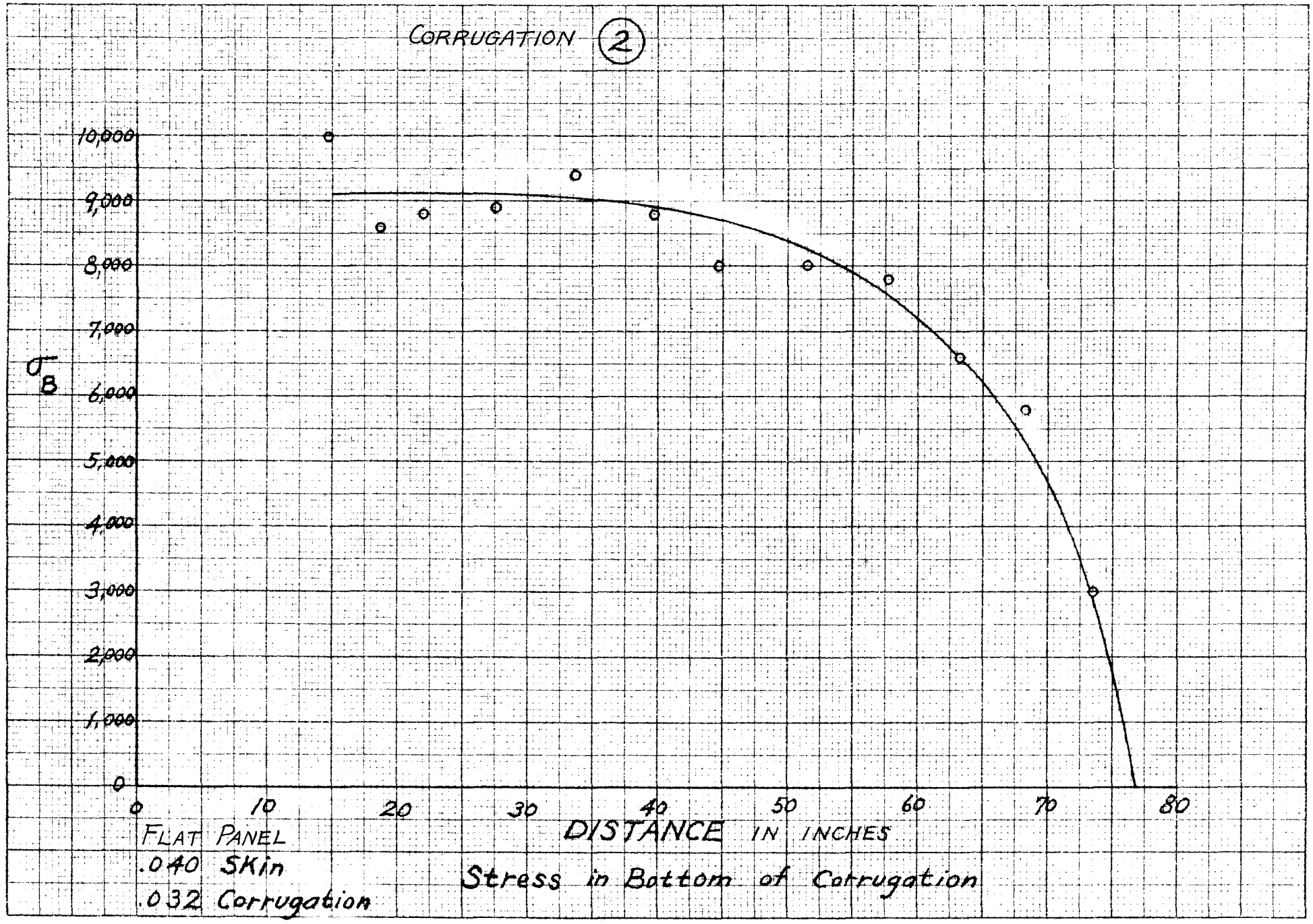
CORRUGATION (2)
10,000
9,000
8,000
7,000
6,000
5,000
4,000
3,000
2,000
1,000
0
σ_B
0
10
20
30
40
50
60
70
80
DISTANCE IN INCHES
FLAT PANEL
.040 SKin
.032 Corrugation
Stress in Bottom of Corrugation

FIG. 14

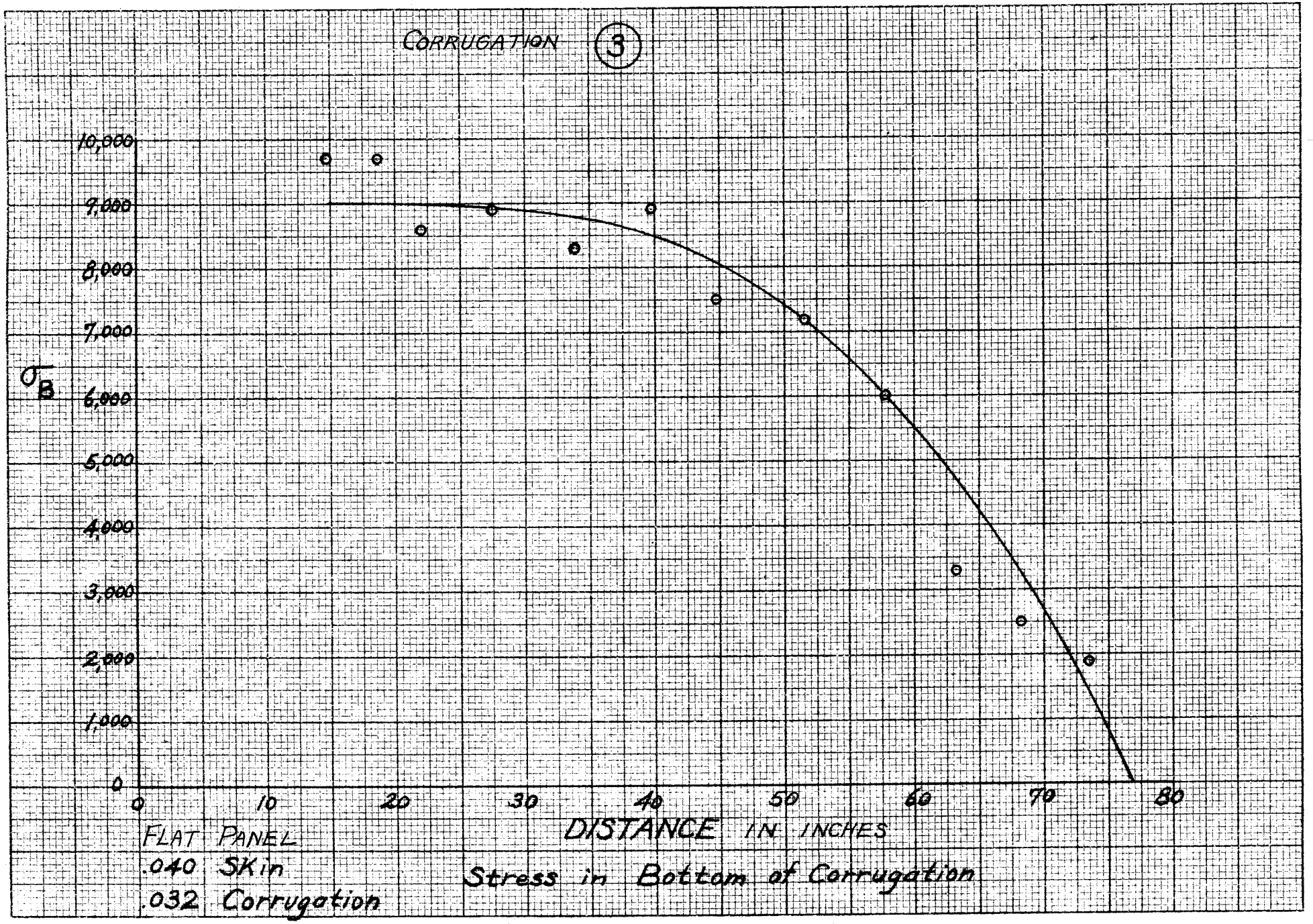
CORRUGATION 3
10,000
9,000
8,000
7,000
σ_B
6,000
5,000
4,000
3,000
2,000
1,000
0
0
10
20
30
40
50
60
70
80
DISTANCE IN INCHES
FLAT PANEL
.040 SKin
.032 Corrugation
Stress in Bottom of Corrugation

FIG. 15

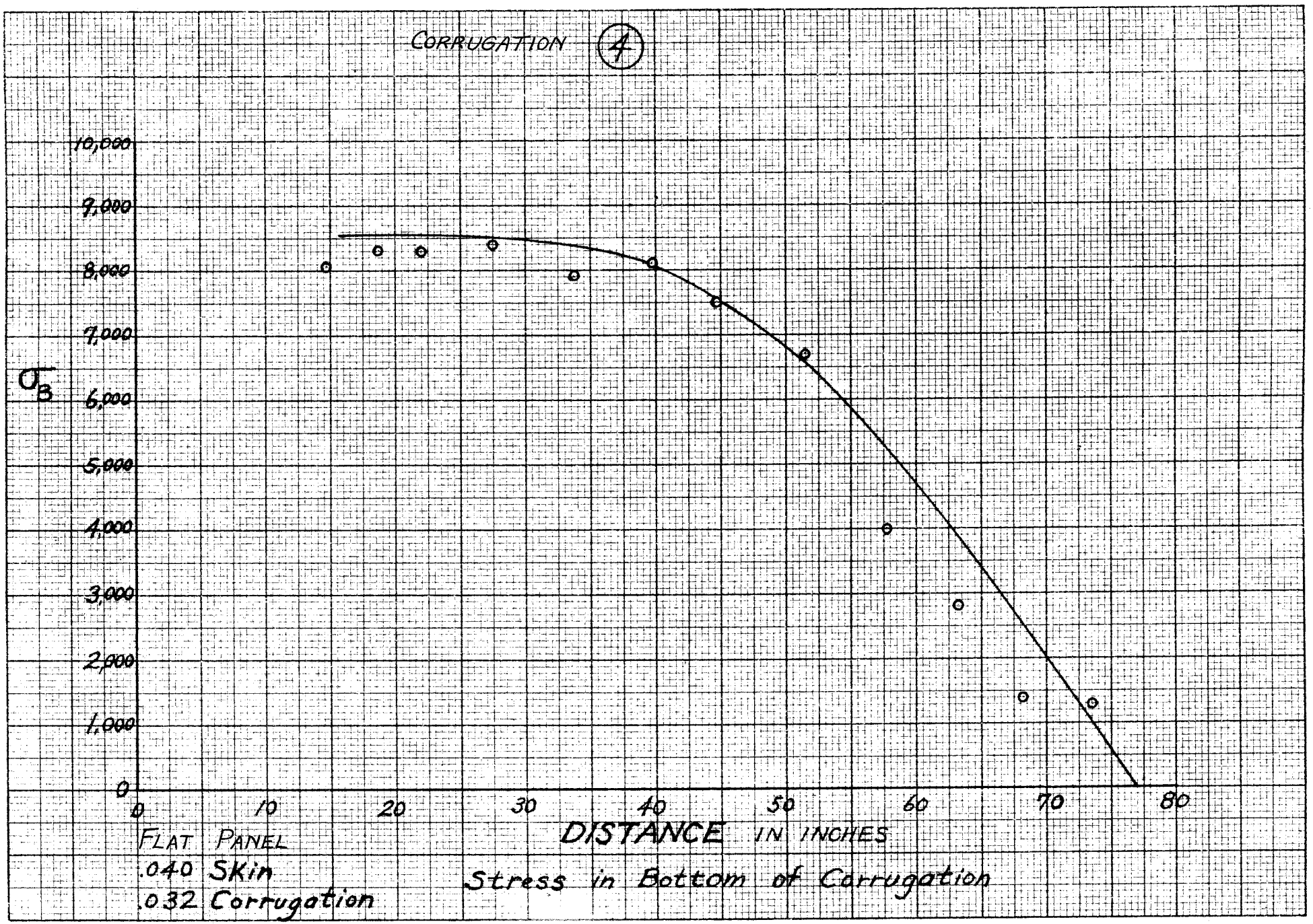
CORRUGATION 4
10,000
9,000
8,000
7,000
σ_B
6,000
5,000
4,000
3,000
2,000
1,000
0
0
10
20
30
40
50
60
70
80
DISTANCE IN INCHES
FLAT PANEL
.040 SKin
.032 Corrugation
Stress in Bottom of Corrugation

FIG. 16

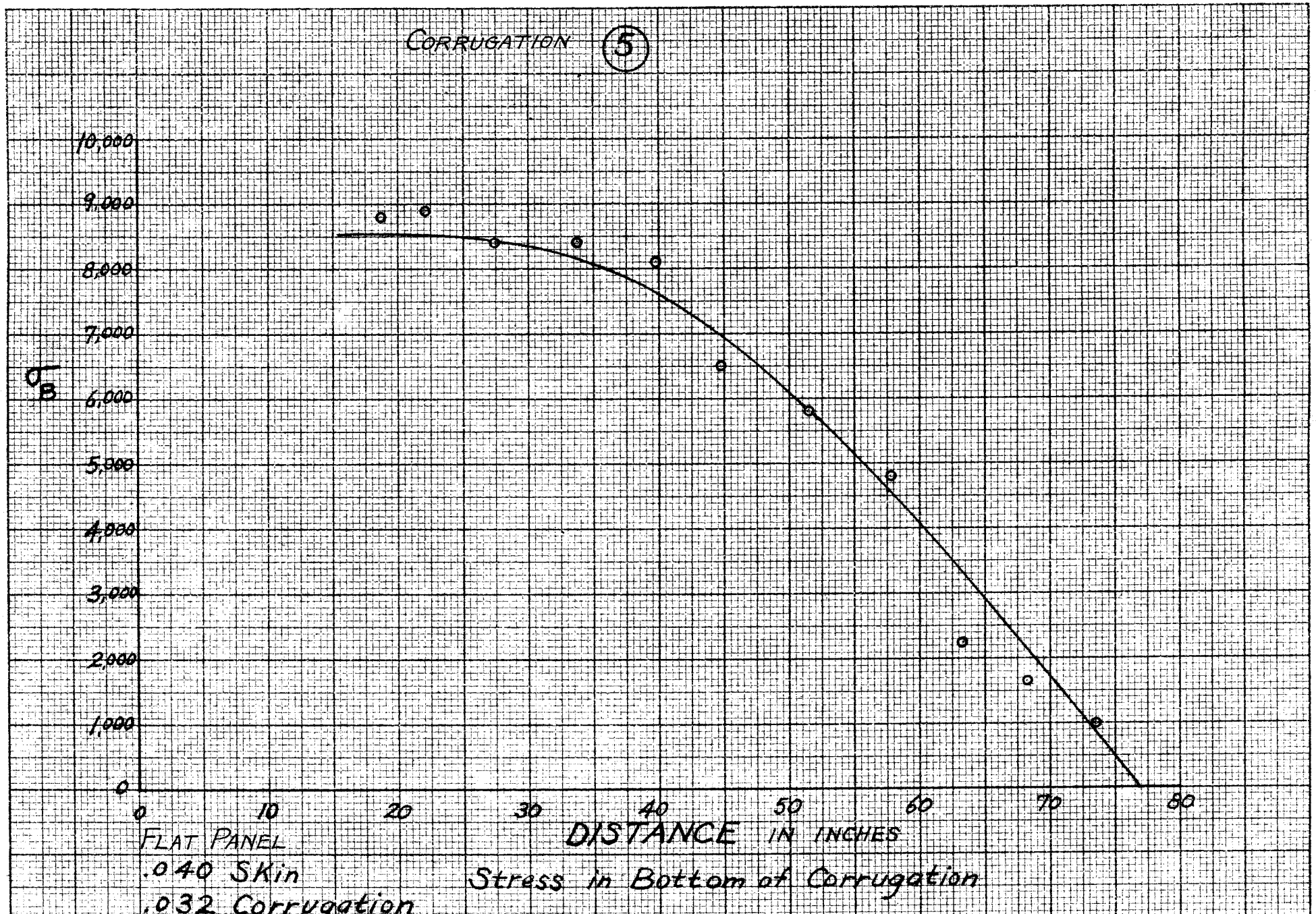
CORRUGATION (5)
10,000
9,000
8,000
7,000
σ_B
6,000
5,000
4,000
3,000
2,000
1,000
0
0
10
20
30
40
50
60
70
80
DISTANCE IN INCHES
FLAT PANEL
.040 SKin
.032 Corrugation
Stress in Bottom of Corrugation

FIG. 17

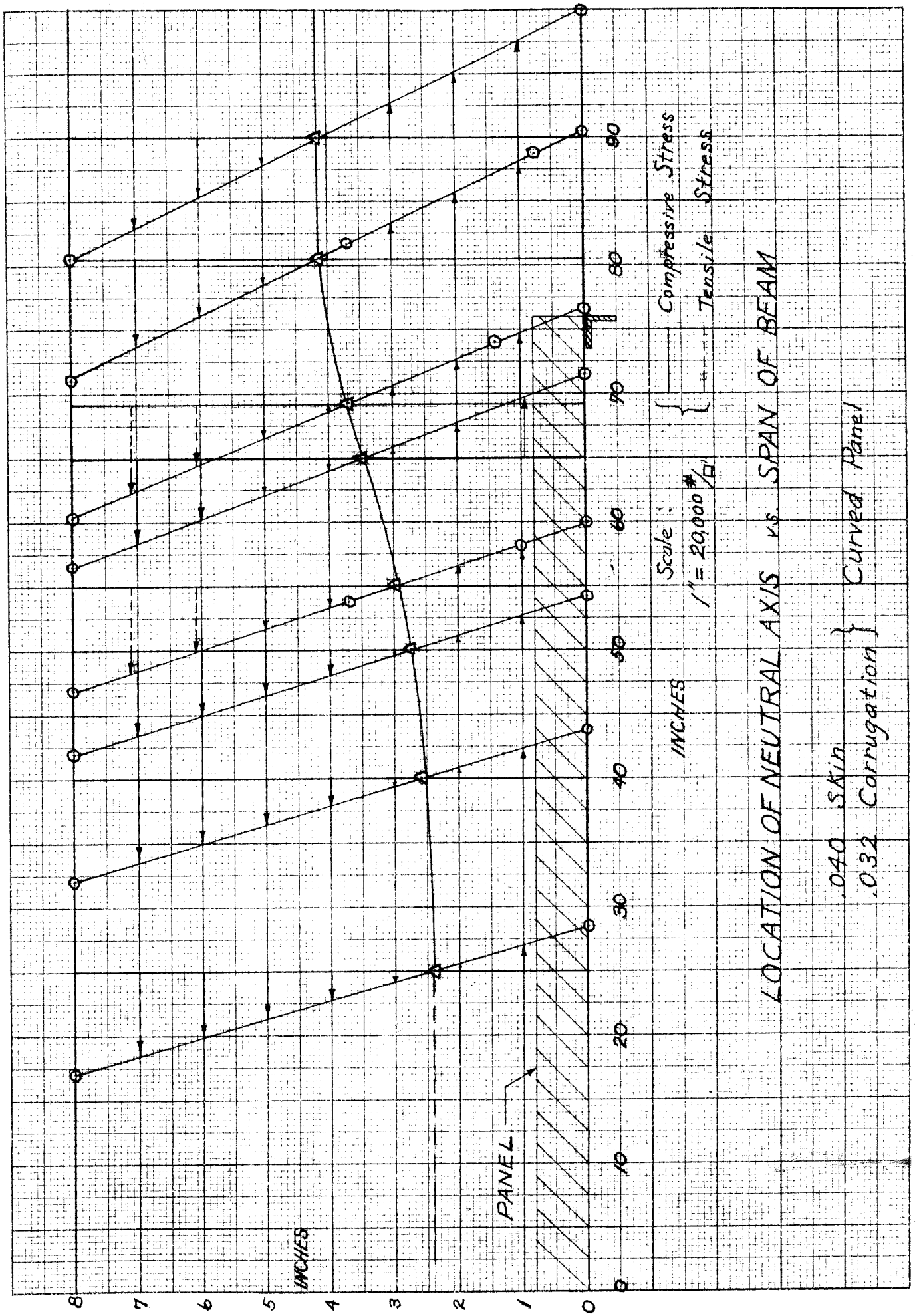
LOCATION OF NEUTRAL AXIS vs. SPAN OF BEAM
.040 Skin
.032 Corrugation
Curved Panel
Scale
1" = 20,000 #/□"
Compressive Stress
Tensile Stress
INCHES
PANEL
INCHES
0
10
20
30
40
50
60
70
80
90
0
1
2
3
4
5
6
7
8

FIG. 18

FLAT PANEL

.040 Skin

.032 Corrugation

STATION 60

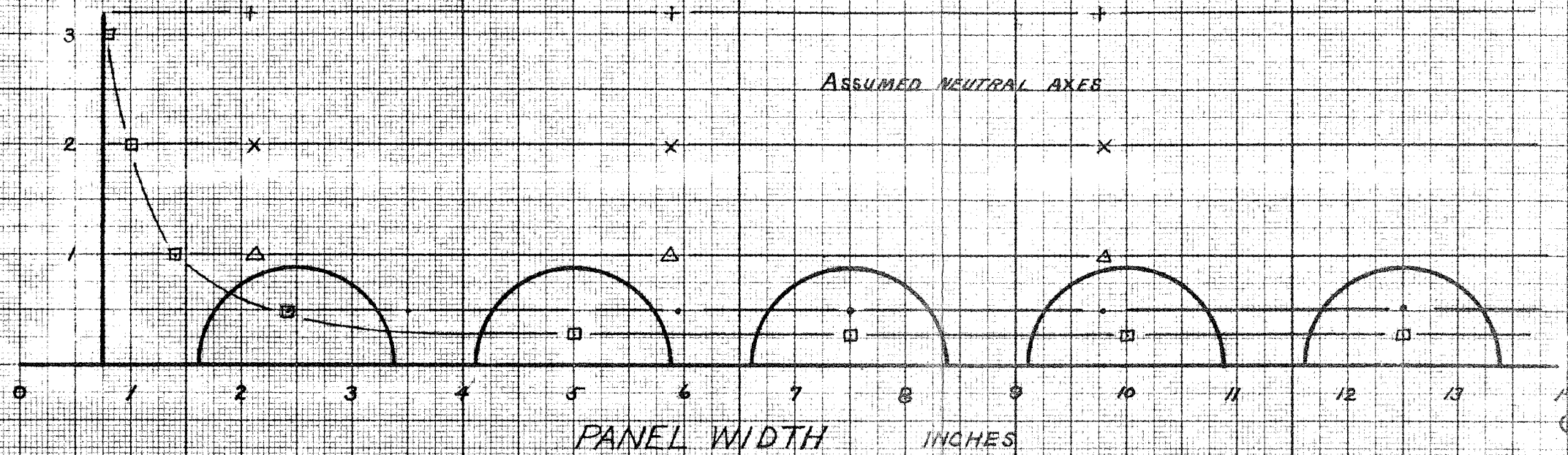

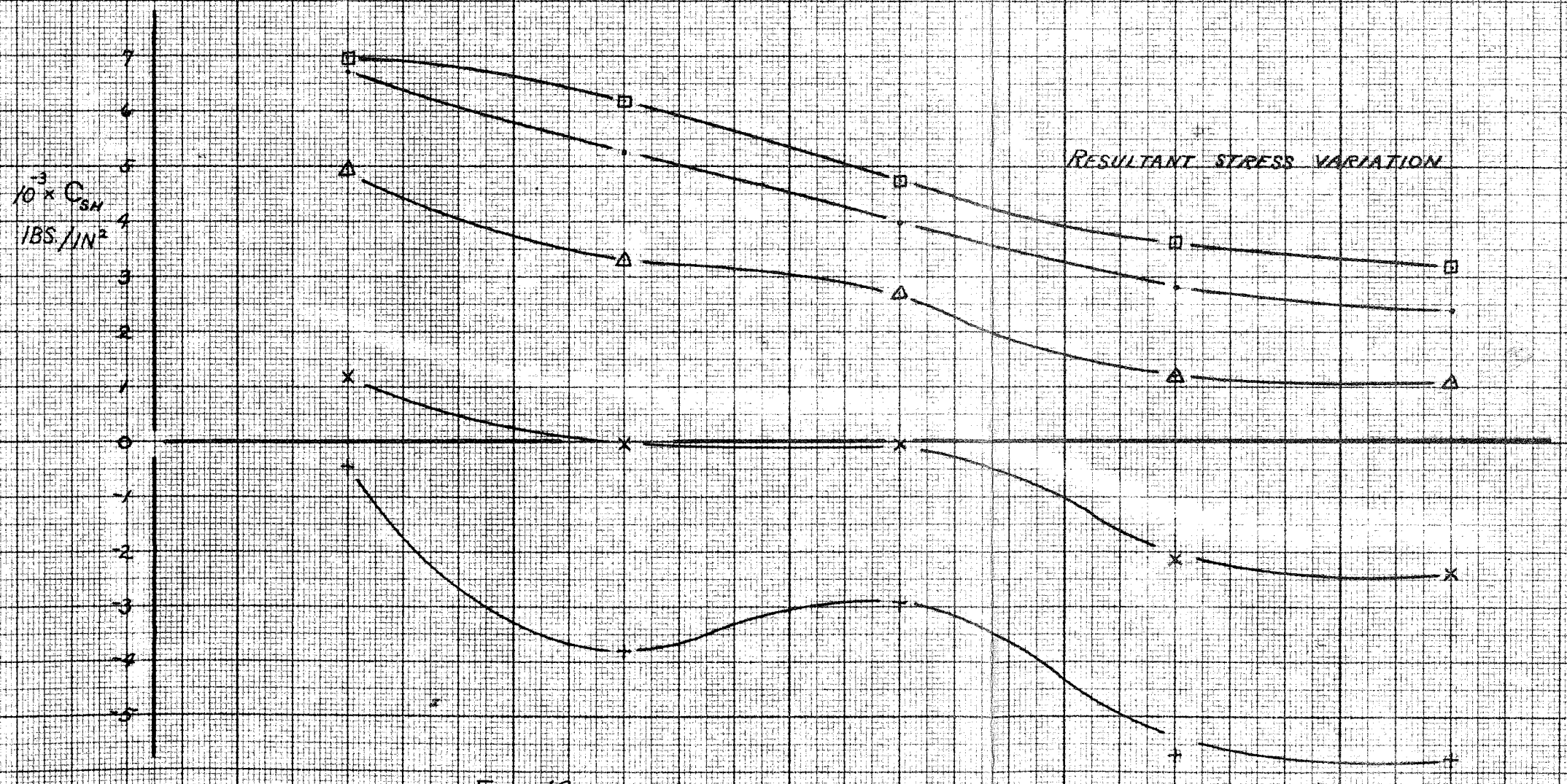

FIG. 19

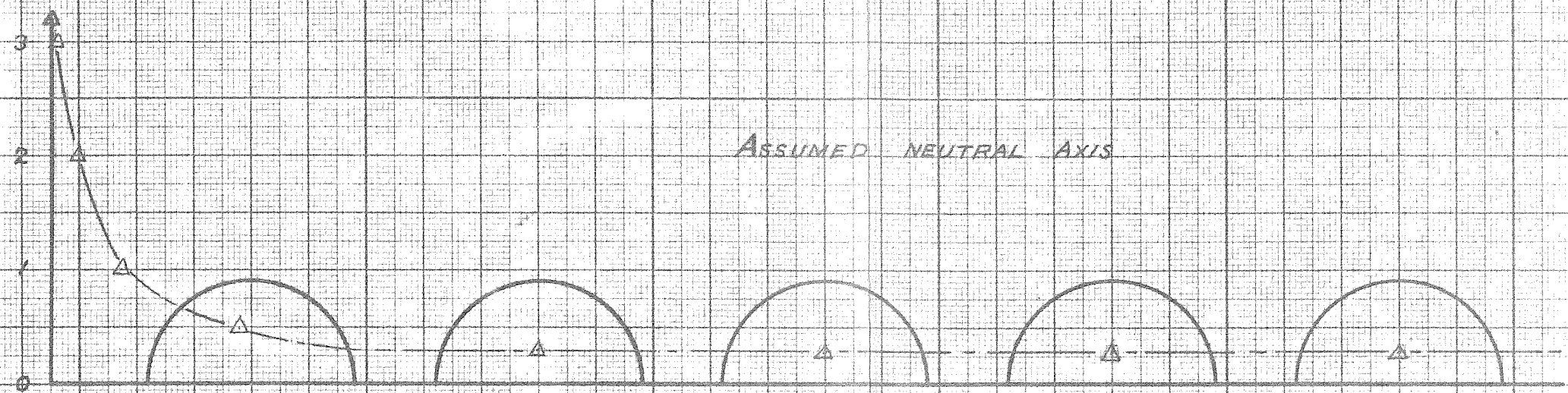

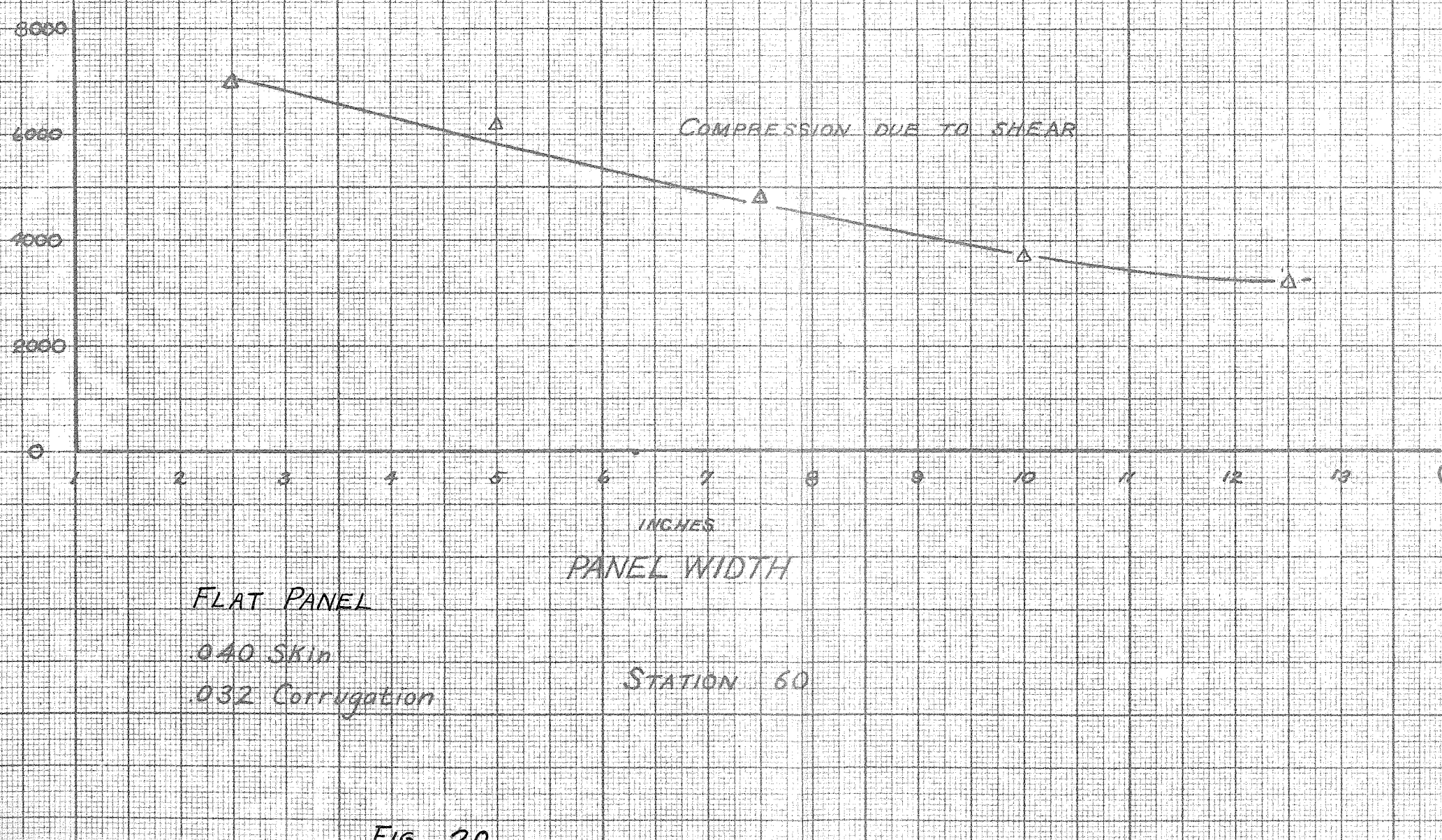

FLAT PANEL

.040 Skin

.032 Corrugation

STATION 60

FIG. 20

CURVED PANEL

.040 SKIN

.032 CORRUGATION

STATION 60

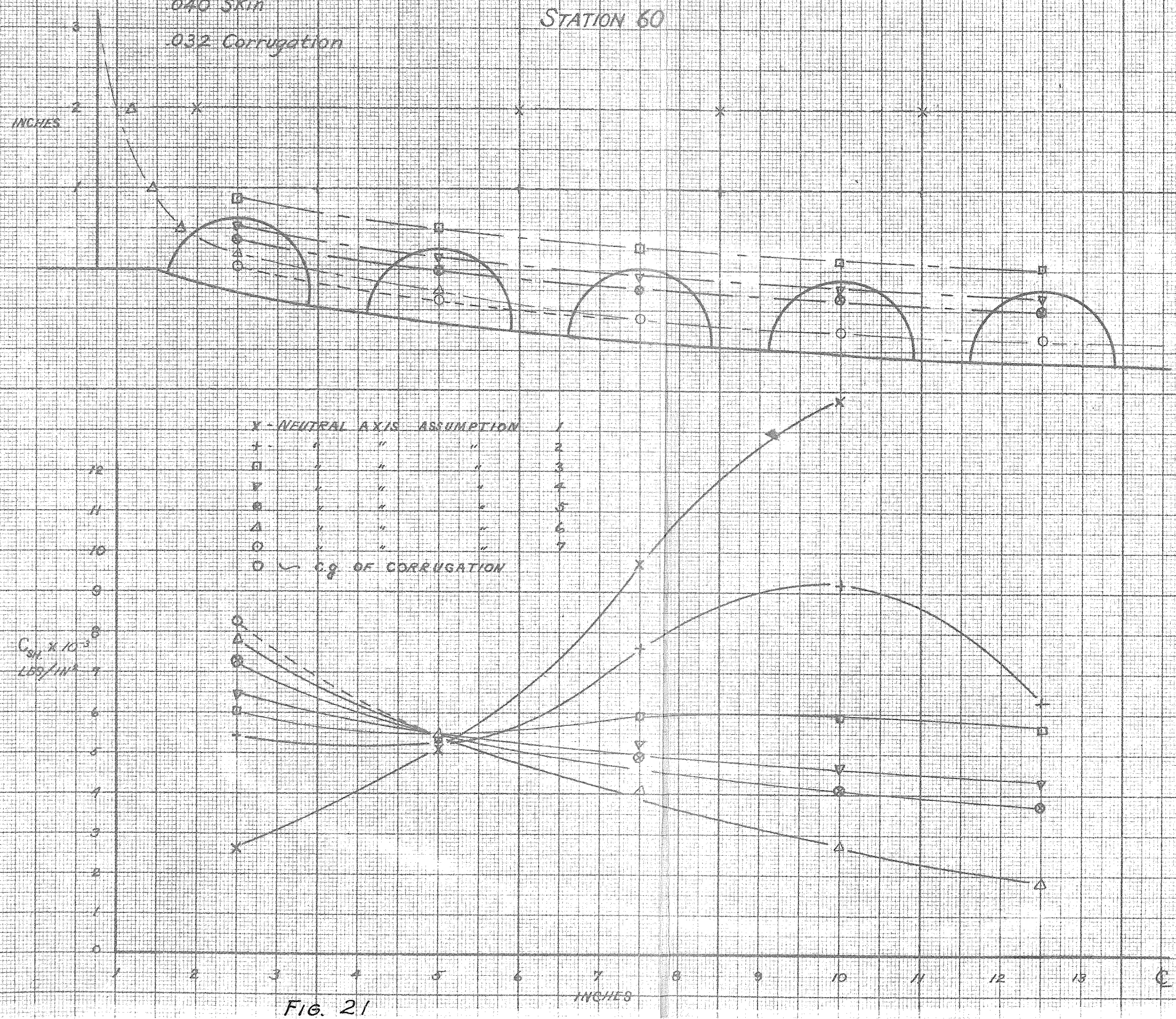

FIG. 21

STATION 50

.032 CORRUGATION
.040 SKIN CURVED

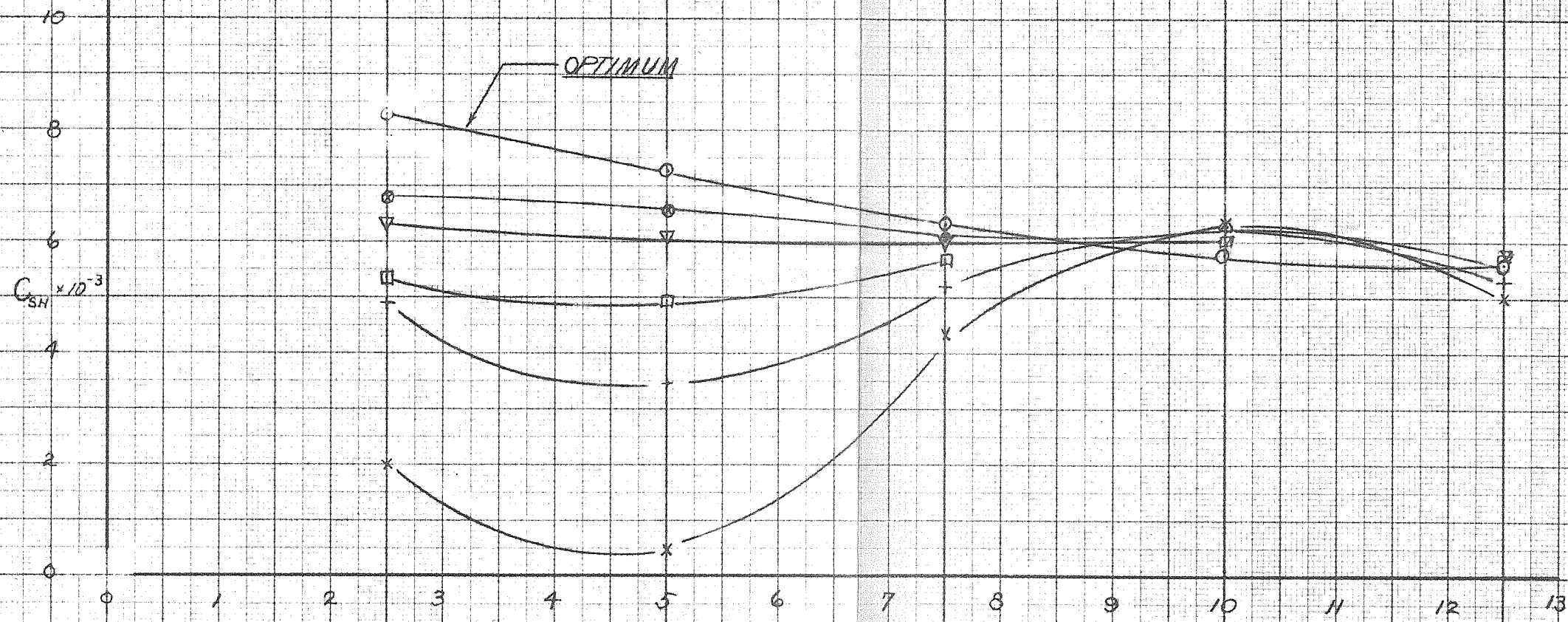

FIG. 22

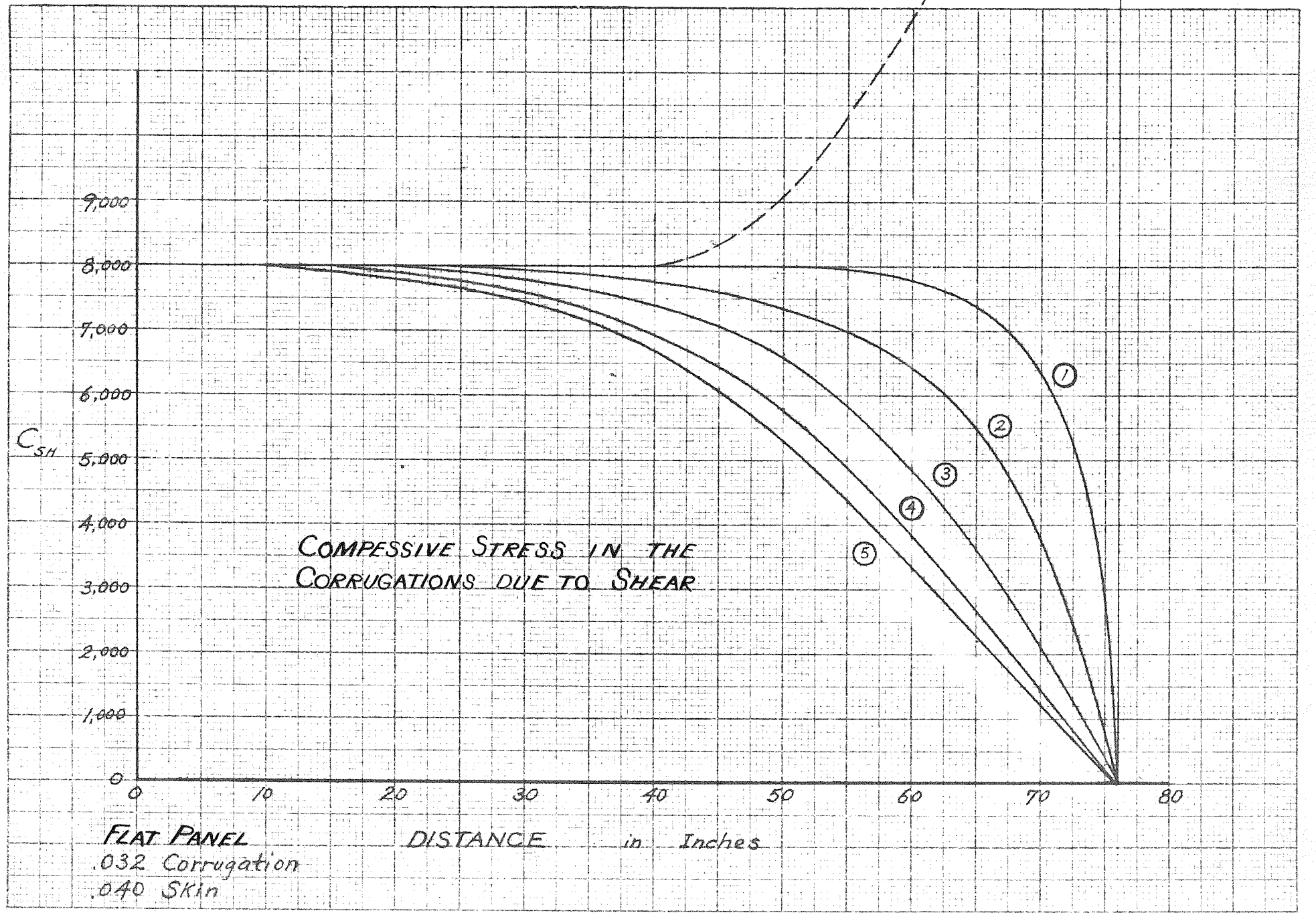
9,000
8,000
7,000
6,000
C_{SH}
5,000
4,000
3,000
2,000
1,000
0
0
10
20
30
40
50
60
70
80
1
2
3
4
5
COMPESSIVE STRESS IN THE
CORRUGATIONS DUE TO SHEAR
FLAT PANEL
.032 Corrugation
.040 Skin
DISTANCE in Inches

FIG. 23

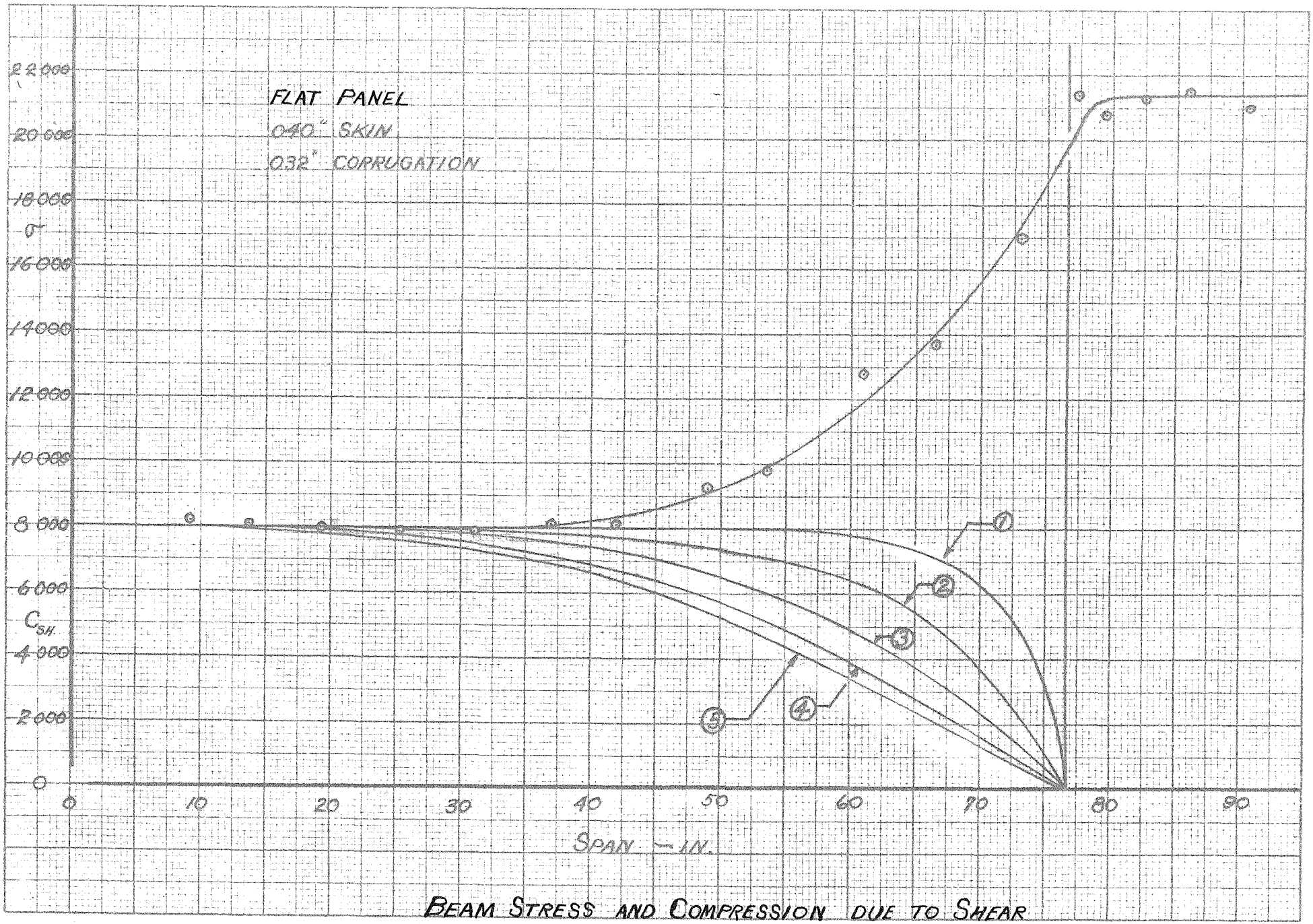

BEAM STRESS AND COMPRESSION DUE TO SHEAR

FIG. 24

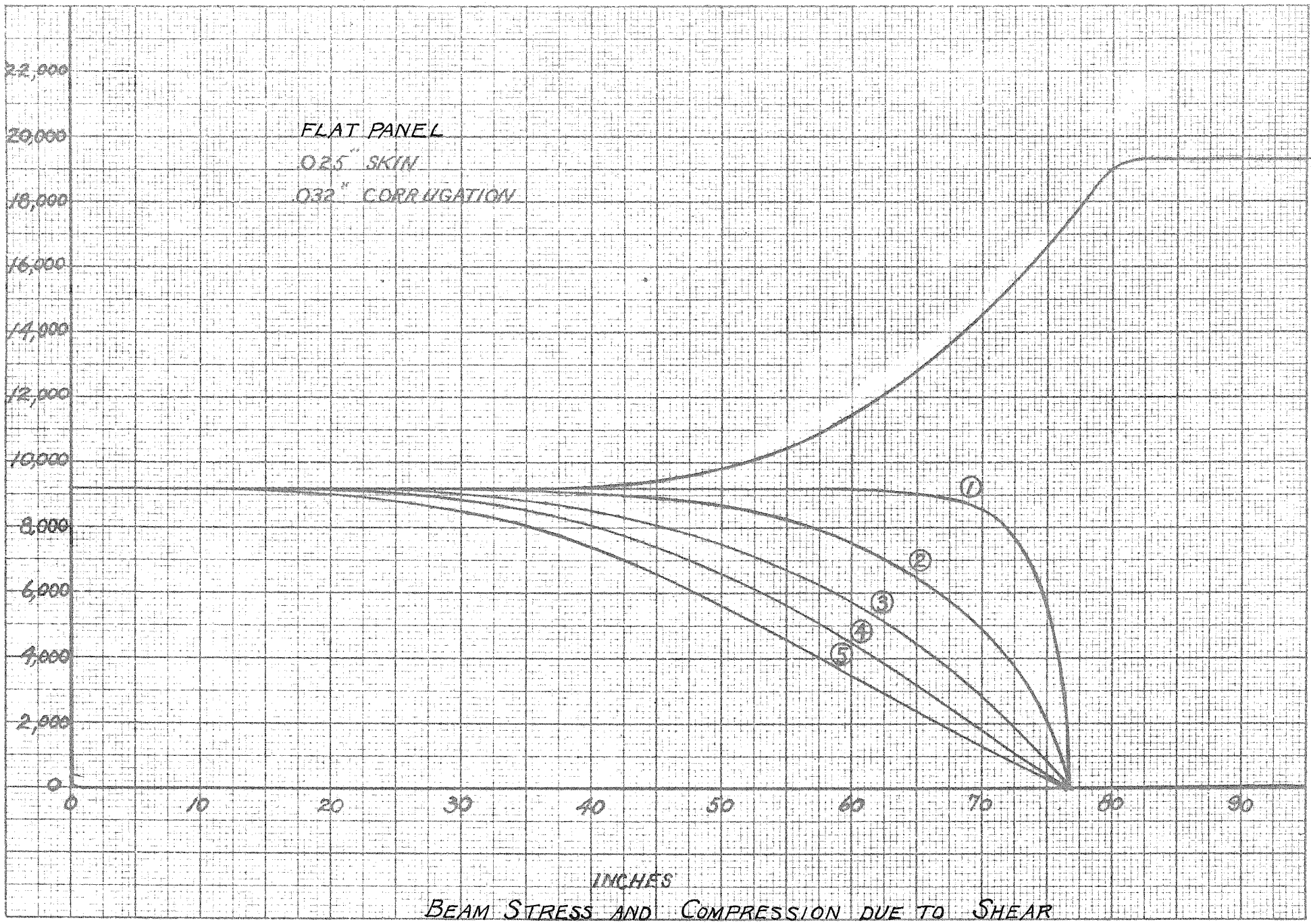

BEAM STRESS AND COMPRESSION DUE TO SHEAR

FIG. 25

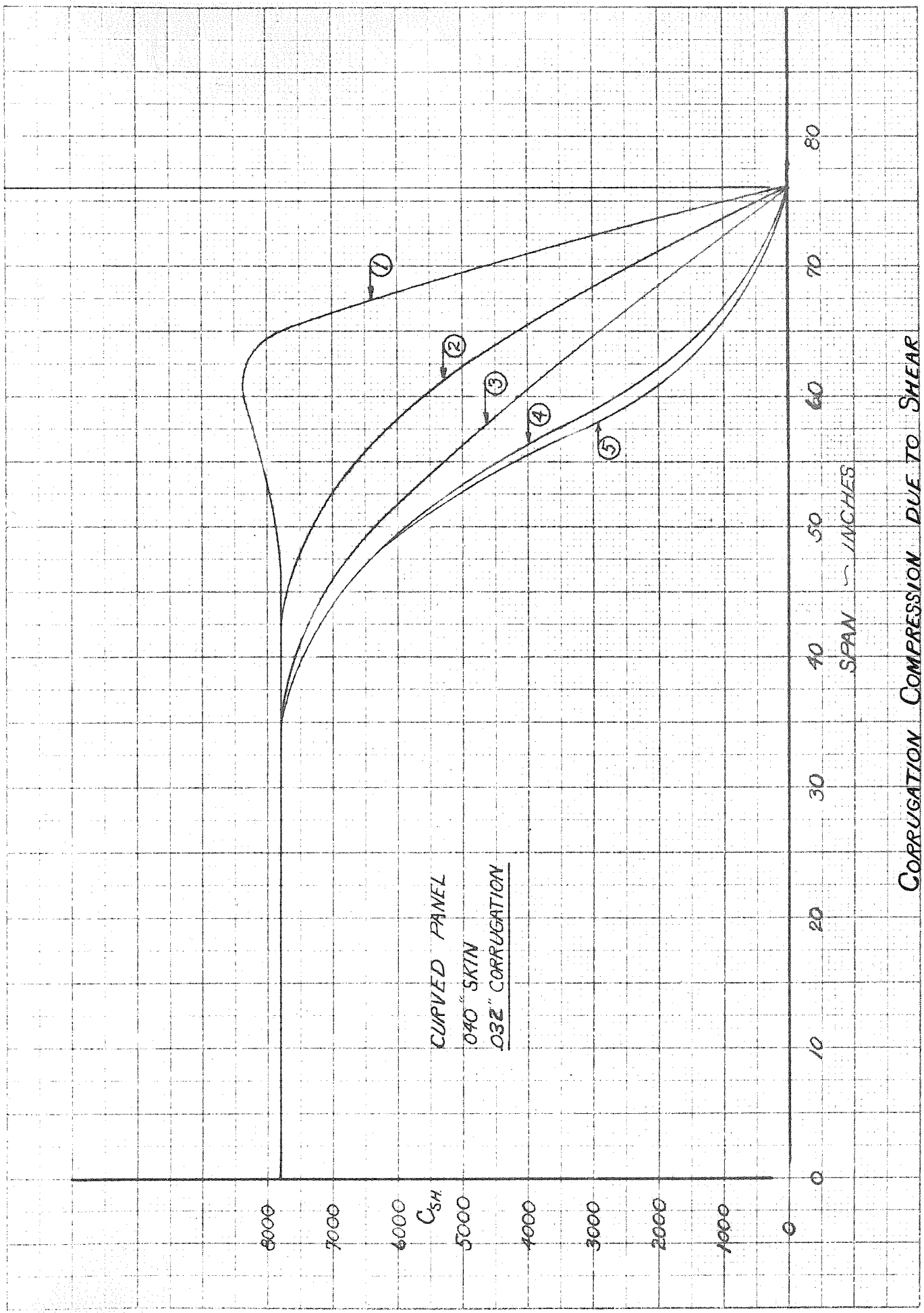

CORRUGATION COMPRESSION DUE TO SHEAR

FIG. 26

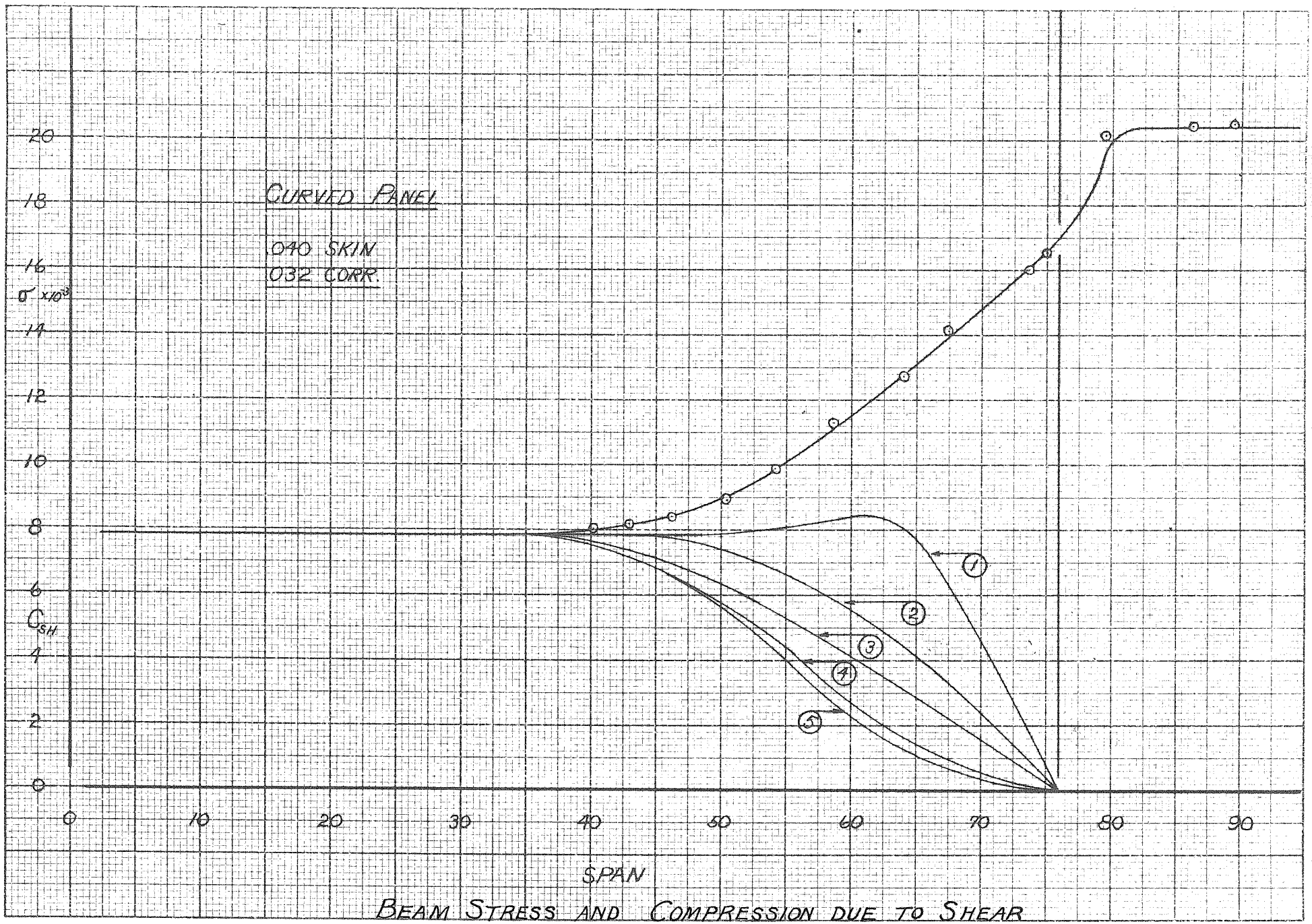

BEAM STRESS AND COMPRESSION DUE TO SHEAR

FIG. 27

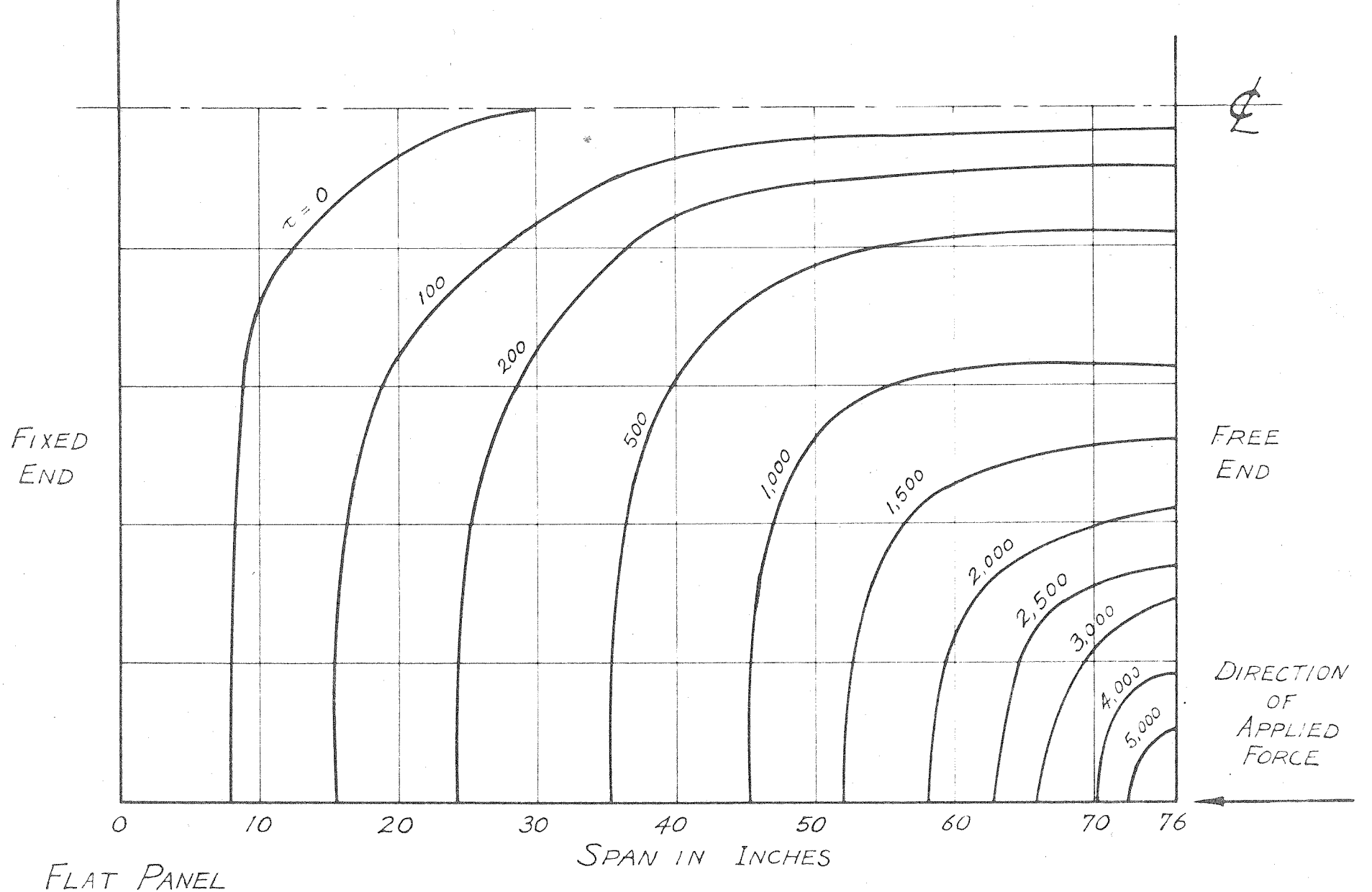

FLAT PANEL
0.040" SKIN
0.032" CORRUGATION

CONTOUR MAP OF SHEARING STRESS LBS./IN²

FIG. 28

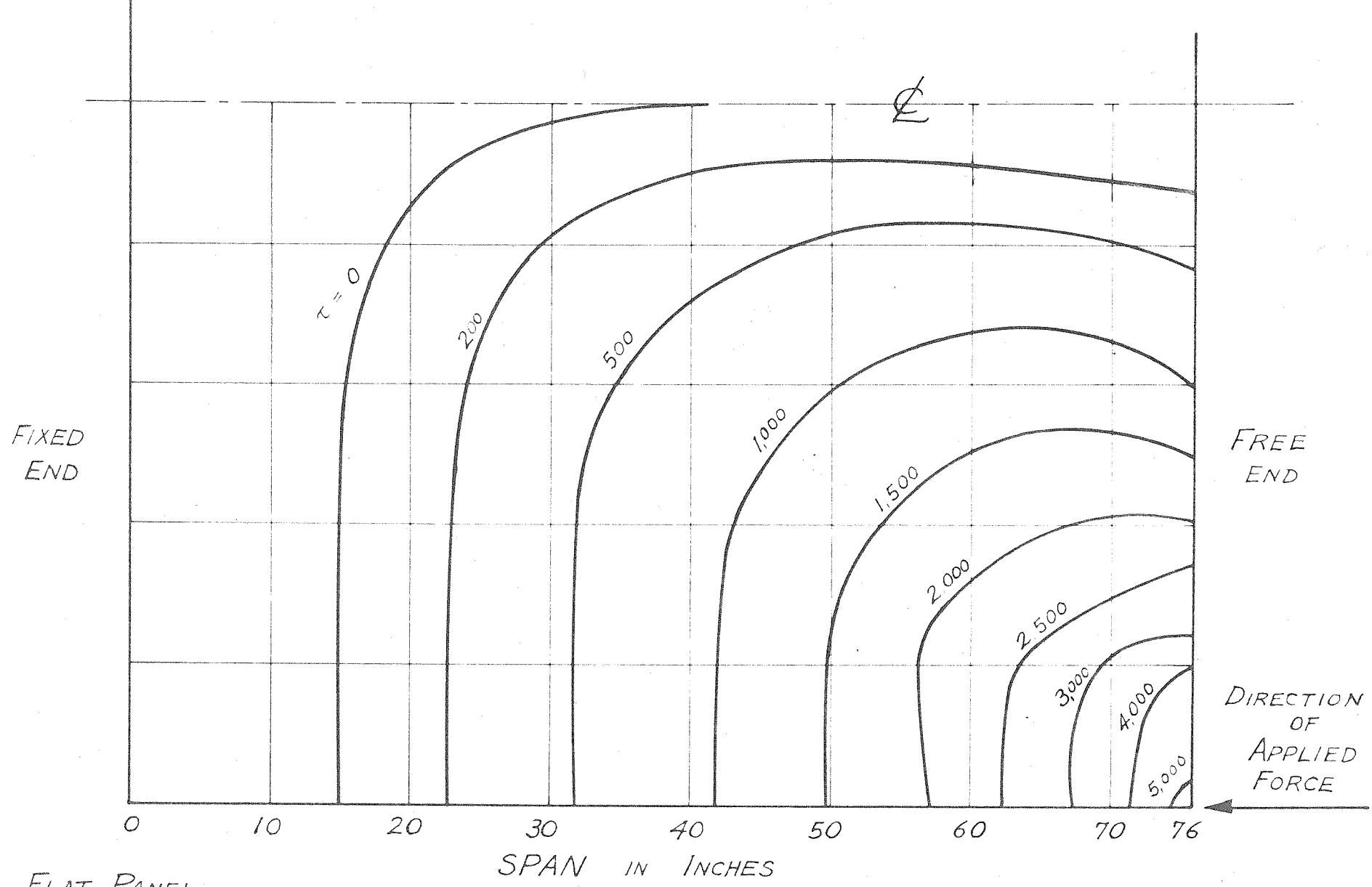

FLAT PANEL
0.025" SKIN
0.032" CORRUGATION

CONTOUR MAP OF SHEARING STRESS LBS./IN.²

FIG. 29

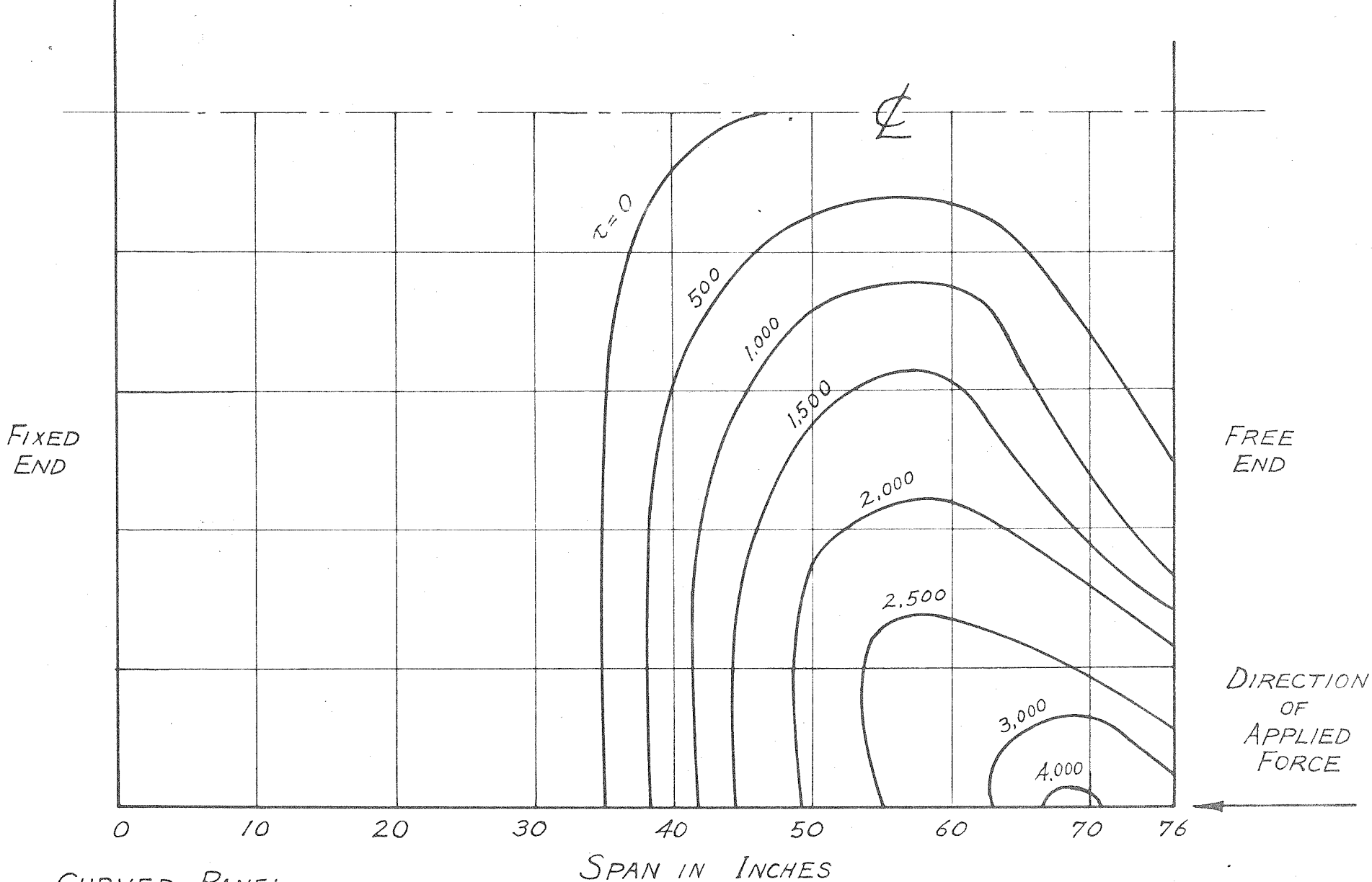

CURVED PANEL
0.040" SKIN
0.032" CORRUGATION

CONTOUR MAP OF SHEARING STRESS $^{LBS}/_{IN.^2}$

FIG. 30

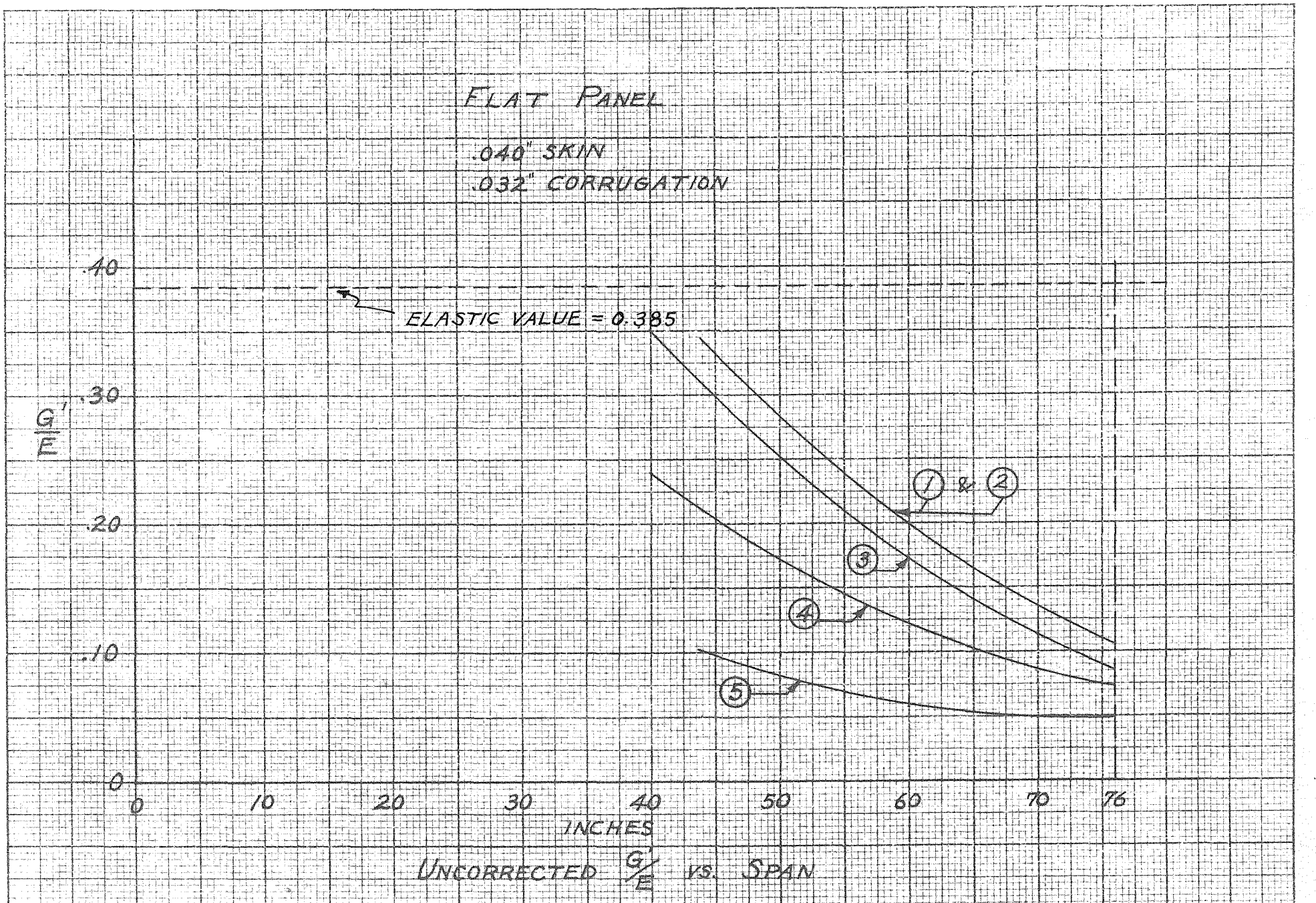
FLAT PANEL
.040" SKIN
.032" CORRUGATION
.40
ELASTIC VALUE = 0.385
.30
G'/E
.20
.10
0
1 & 2
3
4
5
0
10
20
30
40
50
60
70
76
INCHES
UNCORRECTED G'/E VS. SPAN

FIG. 31.

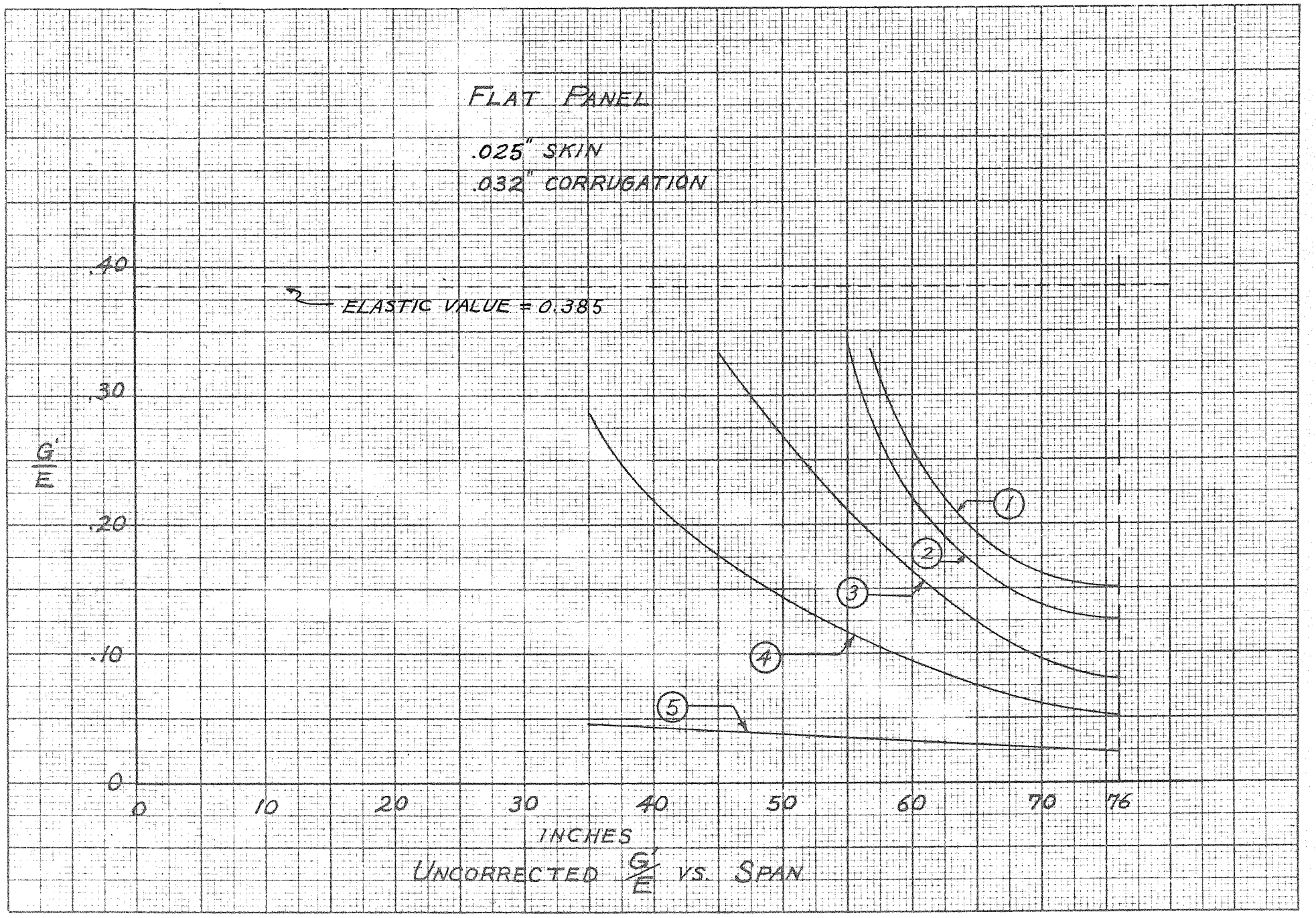
FLAT PANEL
.025" SKIN
.032" CORRUGATION
.40
ELASTIC VALUE = 0.385
.30
G'/E
.20
.10
0
1
2
3
4
5
0
10
20
30
40
50
60
70
76
INCHES
UNCORRECTED G'/E VS. SPAN

FIG. 32

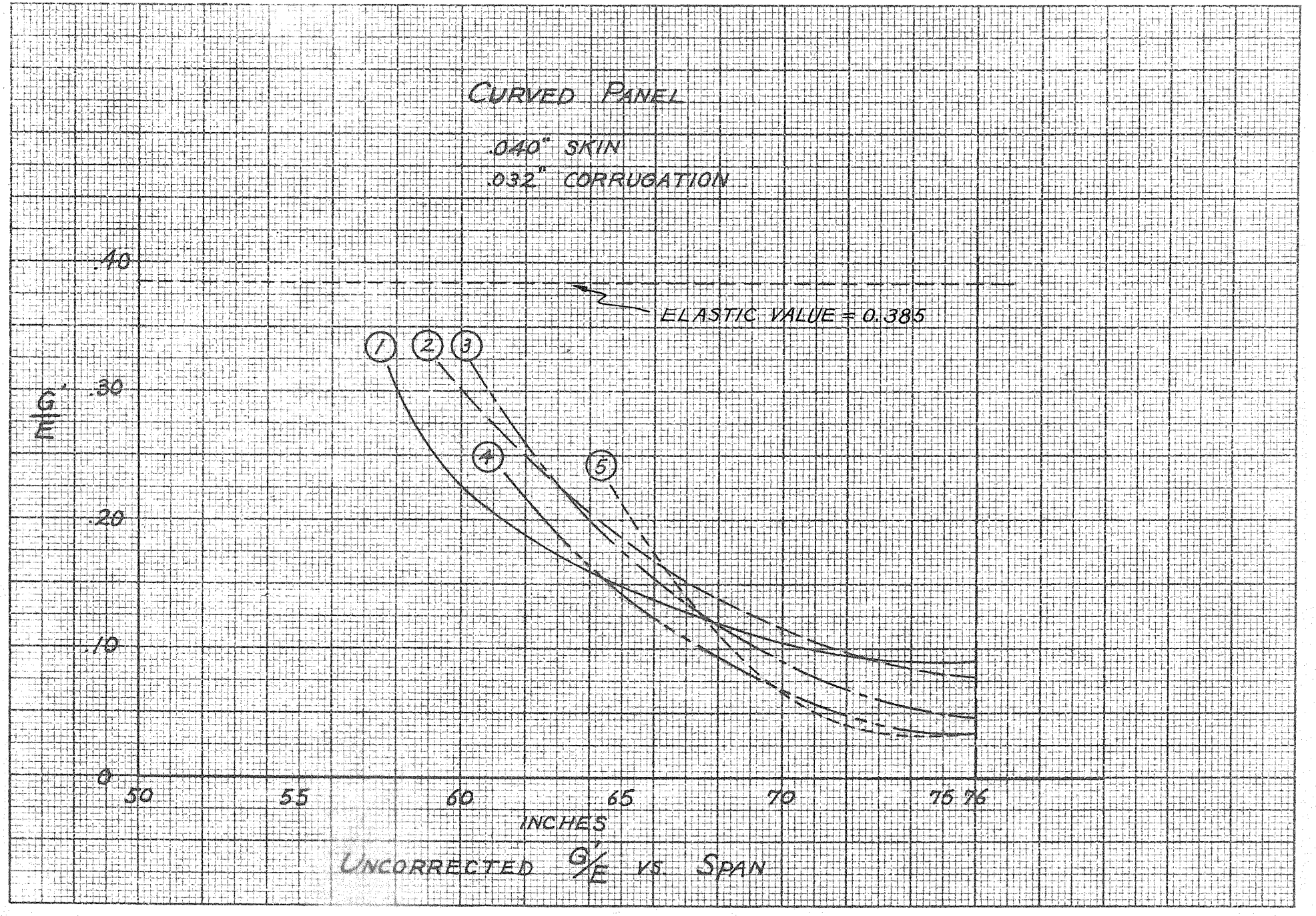
CURVED PANEL
.040" SKIN
.032" CORRUGATION
.40
ELASTIC VALUE = 0.385
1
2
3
4
5
G'/E
.30
.20
.10
0
50
55
60
65
70
75 76
INCHES
UNCORRECTED G'/E VS. SPAN

FIG. 33

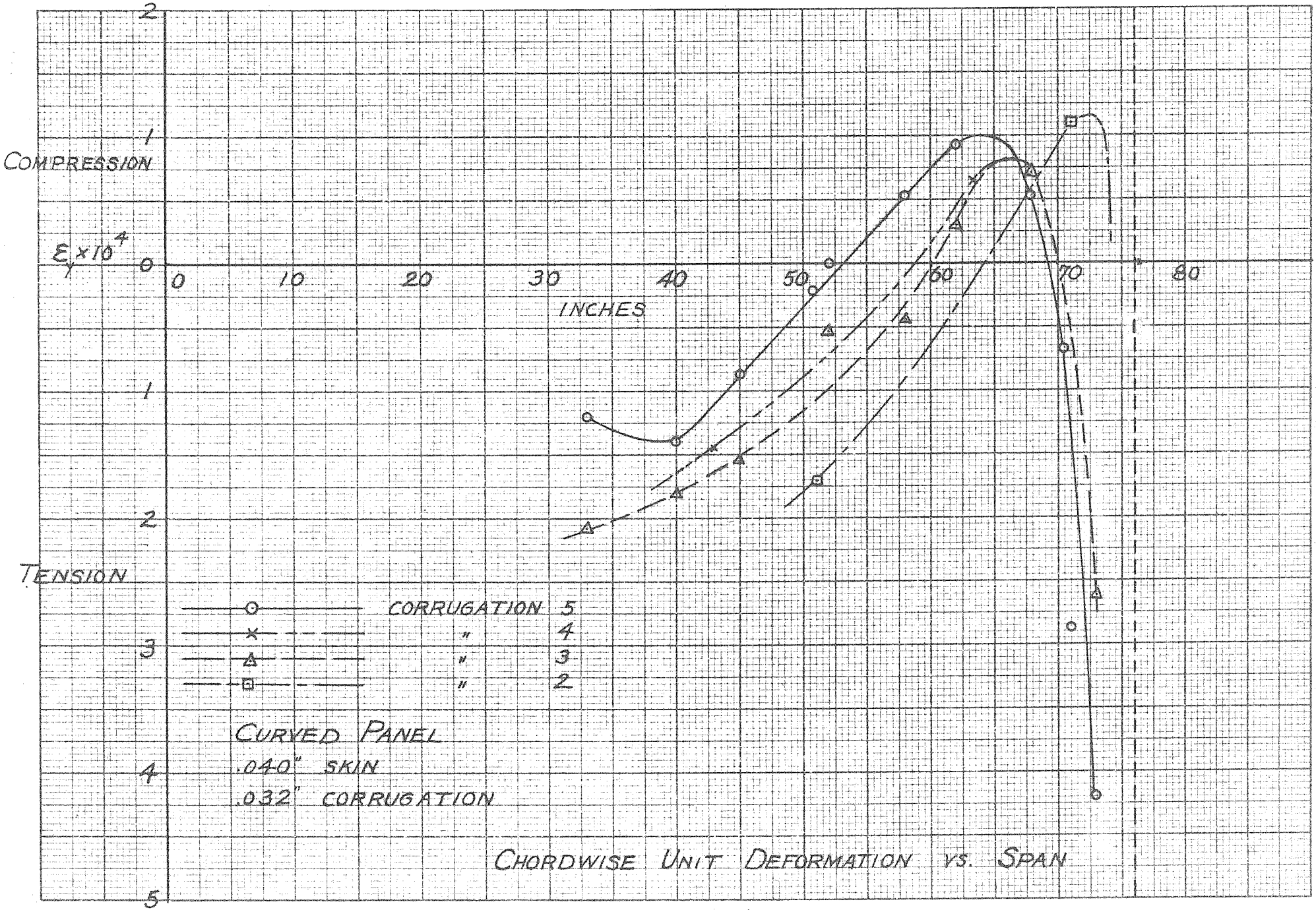
2
1
COMPRESSION
$\varepsilon_y \times 10^4$
0
0
10
20
30
40
50
60
70
80
INCHES
1
2
TENSION
3
CORRUGATION 5
" 4
" 3
" 2
CURVED PANEL
.040" SKIN
.032" CORRUGATION
4
5
CHORDWISE UNIT DEFORMATION VS. SPAN

FIG. 33 A

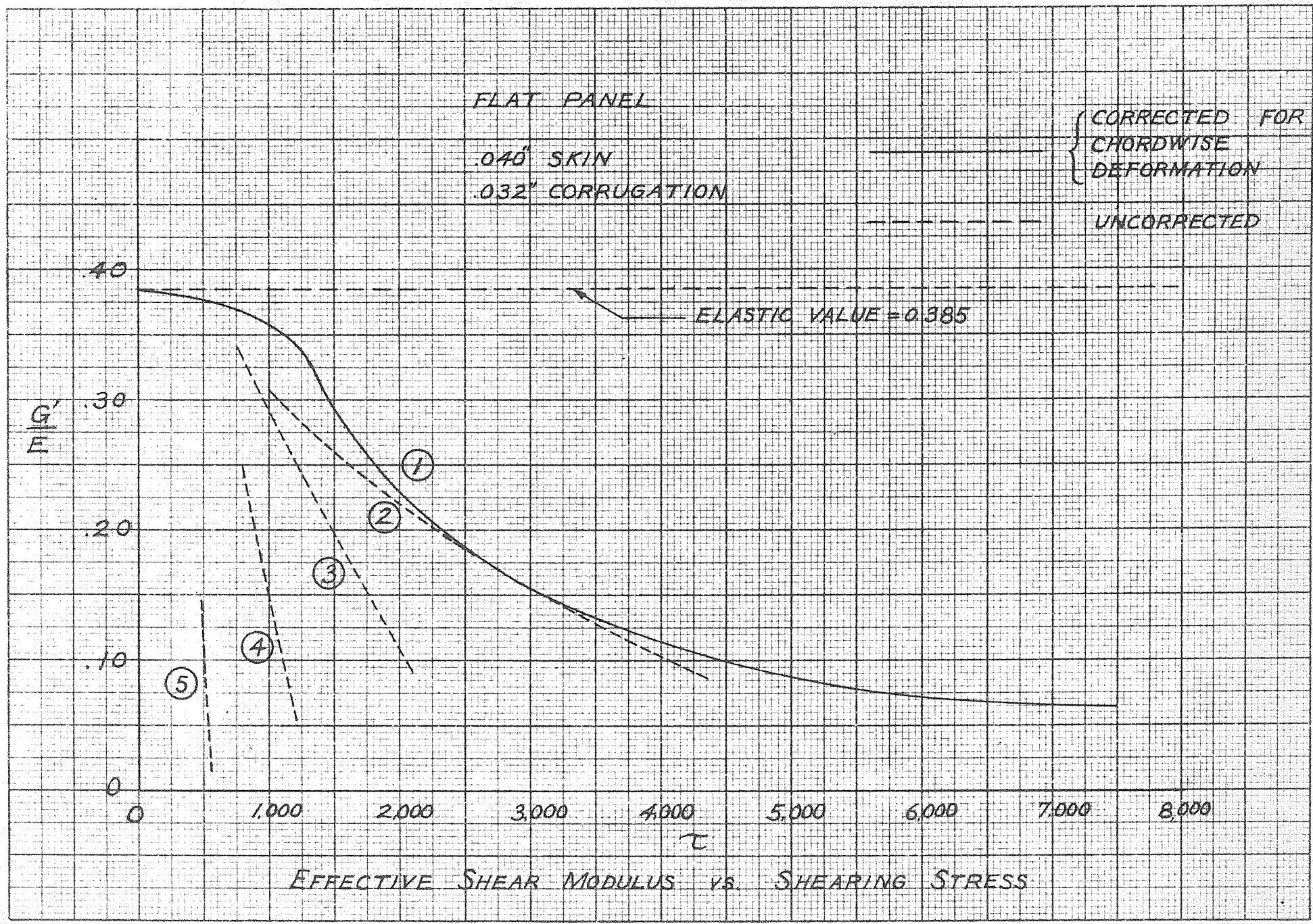
FLAT PANEL
.040" SKIN
.032" CORRUGATION
CORRECTED FOR CHORDWISE DEFORMATION
UNCORRECTED
ELASTIC VALUE = 0.385
.40
.30
.20
.10
0
G'/E
1
2
3
4
5
0
1,000
2,000
3,000
4,000
5,000
6,000
7,000
8,000
τ
EFFECTIVE SHEAR MODULUS vs. SHEARING STRESS

FIG. 34

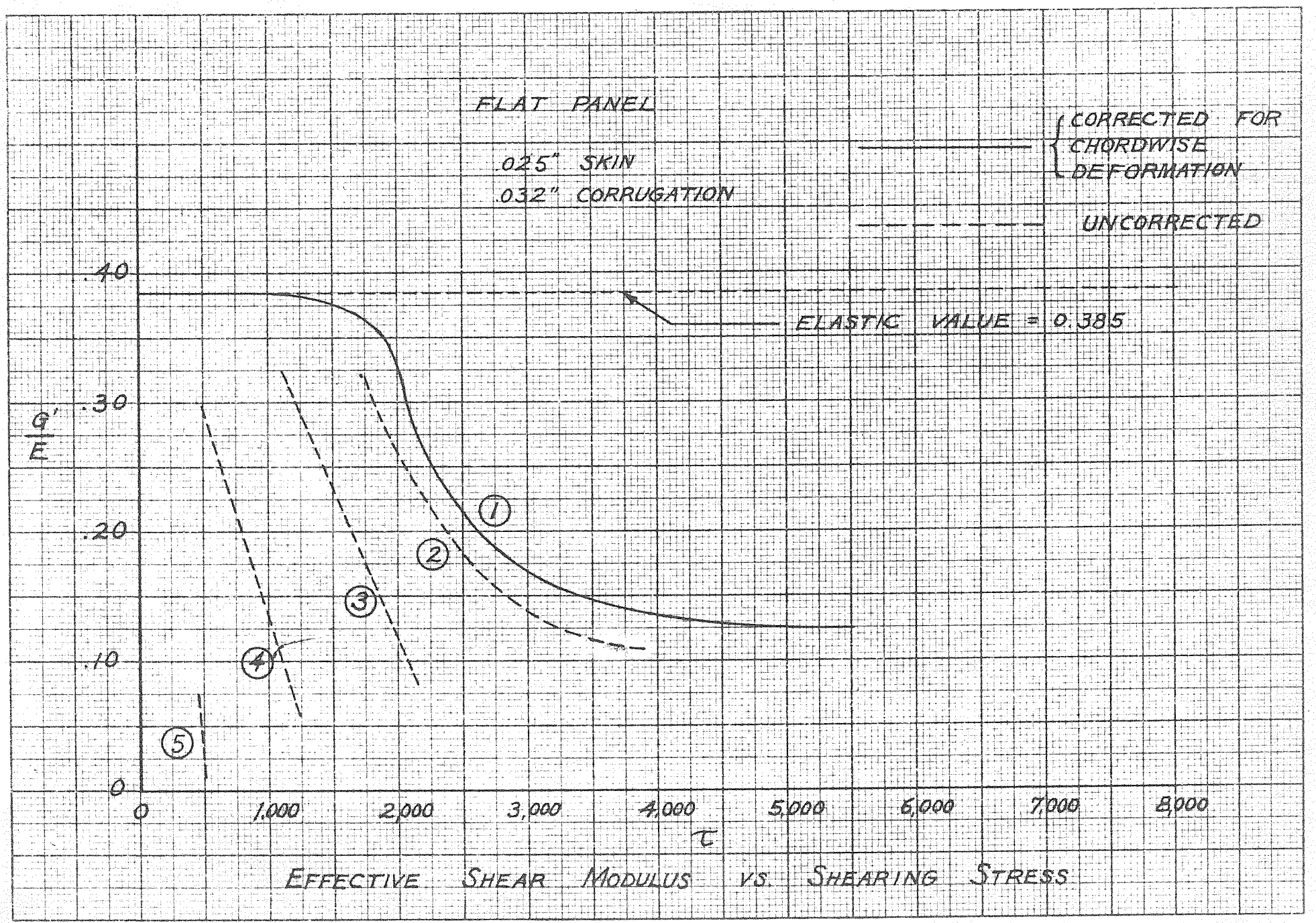
FLAT PANEL
.025" SKIN
.032" CORRUGATION
CORRECTED FOR CHORDWISE DEFORMATION
UNCORRECTED
ELASTIC VALUE = 0.385
G'/E
.40
.30
.20
.10
0
1
2
3
4
5
0
1,000
2,000
3,000
4,000
5,000
6,000
7,000
8,000
τ
EFFECTIVE SHEAR MODULUS VS. SHEARING STRESS

FIG. 35

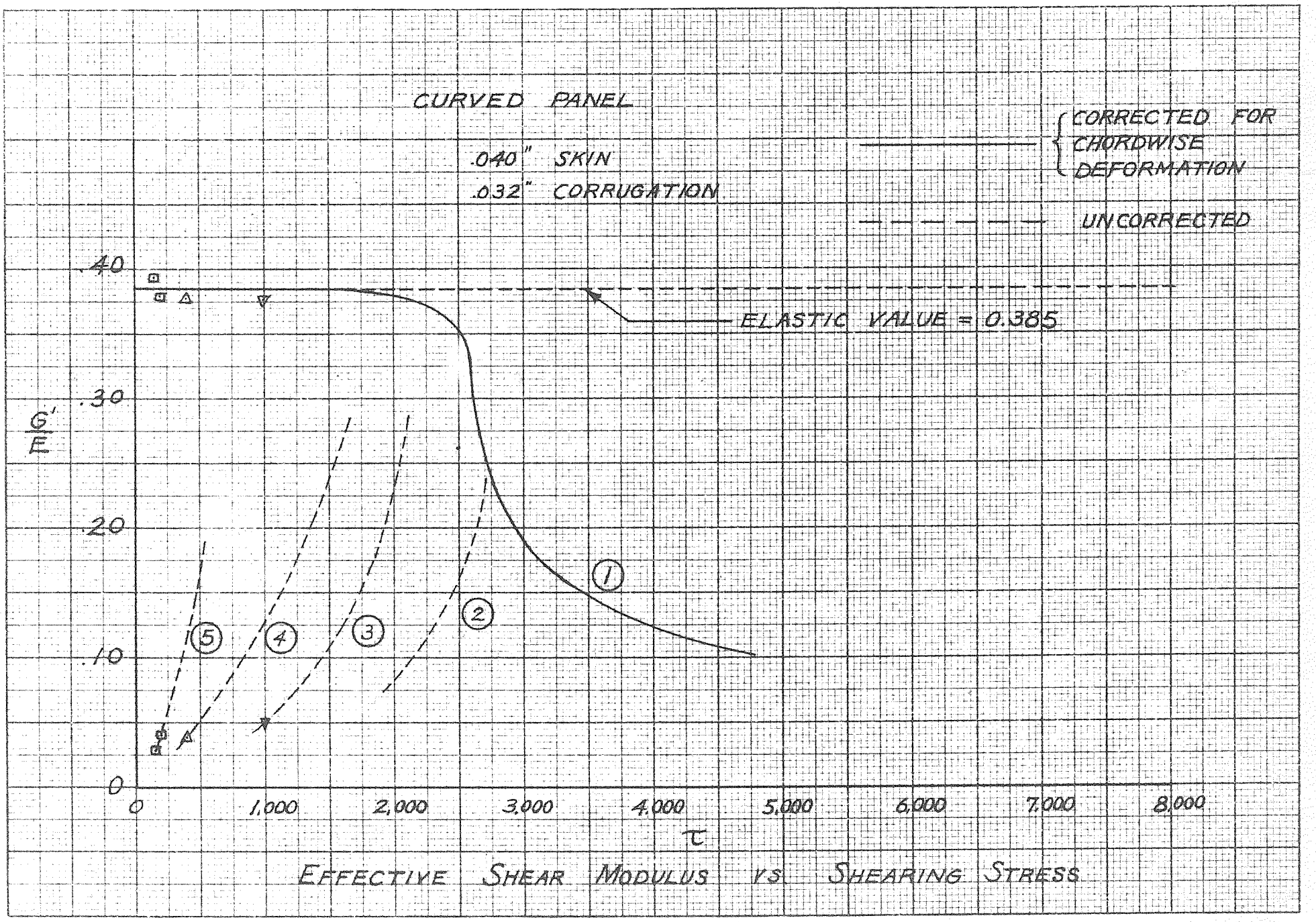
CURVED PANEL
.040" SKIN
.032" CORRUGATION
CORRECTED FOR CHORDWISE DEFORMATION
UNCORRECTED
ELASTIC VALUE = 0.385
G'/E
.40
.30
.20
.10
0
0
1,000
2,000
3,000
4,000
5,000
6,000
7,000
8,000
τ
1
2
3
4
5
EFFECTIVE SHEAR MODULUS VS SHEARING STRESS

FIG. 36